

Graphene Oxide Modified Pencil Graphite Electrode for the Detection of H₂O₂

by

Joyanta Mistry

A thesis submitted in partial fulfillment of the requirements for the degree of
Master of Science in Chemistry



Khulna University of Engineering & Technology

Khulna 9203, Bangladesh.

June -2018

Declaration

This is to certify that the thesis work entitled “Graphene Oxide Modified Pencil Graphite Electrode for the Detection of Hydrogen per Oxide” has been carried out by Joyanta Mistry in the Department of Chemistry, Khulna University of Engineering & Technology, Khulna, Bangladesh. The above thesis work has not been submitted anywhere for the award of any degree or diploma.



Signature of Supervisor


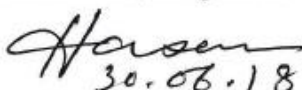


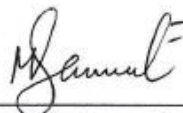


Signature of Candidate

Approval

This is to certify that the thesis work submitted by Joyanta Mistry with title “**Graphene Oxide Modified Pencil Graphite Electrode for the Detection of H₂O₂**” has been approved by the board of examiners for the partial fulfillment of the requirements for the Degree of Master of Science in the Department of Chemistry, Khulna University of Engineering & Technology, Khulna, Bangladesh in June, 2018.

BOARD OF EXAMINERS

1. 
Dr. A. B. M. Mamun Jamal
Assistant Professor
Department of Chemistry
Khulna University of Engineering & Technology
Khulna-9203, Bangladesh
Chairman
(Supervisor)
2. 
Head
Department of Chemistry
Khulna University of Engineering & Technology
Khulna-9203, Bangladesh
Member
3. 
Dr. Mohammad Abu Yousuf
Professor, Department of Chemistry
Khulna University of Engineering & Technology
Khulna-9203, Bangladesh
Member
4. 
Dr. Md. Mizanur Rahman Badal
Professor, Department of Chemistry
Khulna University of Engineering & Technology
Khulna-9203, Bangladesh
Member
5. 
Dr. Md. Qamrul Ehsan
Professor, Department of Chemistry
University of Dhaka
Dhaka-1000, Bangladesh
Member
(External)

Acknowledgements

Firstly I would like to express my gratitude to my supervisor **Dr. A. B. M. Mamun Jamal**, Assistant Professor, Department of Chemistry, Khulna University of Engineering & Technology, for his endless enthusiasm and support throughout my studies. He had helped me at each and every point of the thesis work with his dedication, comments, suggestions and guidance which put me on the right path to fulfill the requirement, without which this situation was impossible to overcome. He also friendly supported me a lot in my daily life which I truly appreciate.

I would like to thank Prof. Dr. Md. Hasan Morshed, Head, the Department of Chemistry, KUET and the staff of the department for their continuous support during my thesis work. I would like to give my special thanks to Prof. Dr. Mohammad Abu Yousuf, Department of Chemistry, KUET for his excellent support, advice and enthusiasm throughout my M.Sc. I would like to thanks University Grant Commission and Khulna University of Engineering & Technology for funding my research.

I also want to express my all thanks, gratefulness and appreciations to my fellow researchers in the department for all the support they have done to me during this one and half year period.

Huge thanks go to my family for giving me inspiration, blessing and encouragement throughout the period of study.

Joyanta Mistry

Abstract

In this work, we propose a new, robust and reliable way to detect H_2O_2 . Reduced graphene oxide-supported tin oxide ($\text{SnO}_2\text{-rGO}$) as electrochemical sensing material has been synthesized and drop casted on pencil graphite electrode (PGE) for the detection of H_2O_2 . Electrochemical characterization has been done using cyclic voltammetry (CV) and amperometry. Hydrothermal synthesis method was used for the fabrication of SnO_2 nanoparticles and GO prepared by modified Hummers method. For the detection of H_2O_2 , the nanoparticles were mixed with Nafion and chitosan before drop coating onto the PGE surface. In this work, we have found a good catalytic activity of $\text{SnO}_2\text{-rGO}$ modified 3B PGE at pH 7.4. Electrochemical studies showed that the sensing platform fabricated using $\text{SnO}_2\text{-rGO}$ possesses fast mass transport, good electrical conductivity and high sensitivity and selectivity for the detection of H_2O_2 . $\text{SnO}_2\text{-GO/PGE}$ exhibited amperometric sensitivity of $53.4 \mu\text{AmM}^{-1}\text{cm}^{-2}$ with a response time 2s, limit of detection of $0.09\mu\text{M}$ ($n=3$), and linearity range of 1-7 mM. The electrode can be prepared simply and at low cost, and present a promising tool for sensing H_2O_2 .

Contents

	PAGE
Title page	i
Declaration	ii
Certificate of Research	iii
Acknowledgement	iv
Abstract	v
Contents	vi
List of Tables	viii
List of Figures	ix

CHAPTER I	Introduction	
	1.1 General	1
	1.2 Basic concept of H ₂ O ₂	3
	1.3 Structure and properties of H ₂ O ₂	4
	1.3.1 Properties	4
	1.3.2 Aqueous solutions	4
	1.3.3 Structure	6
	1.3.4 Comparison with analogues	7
	1.4 Reactions of H ₂ O ₂	8
	1.4.1 Decomposition	8
	1.4.2 Redox reactions	8
	1.4.3 Organic reactions	10
	1.5 Precursor to other peroxide compounds	10
	1.6 Electrochemical sensors	13
	1.7 Chemically modified electrodes	13
	1.7.1 General methods of modification of electrodes	14
	1.8 Fundamentals of electrochemistry	17
	1.9 Electrochemical setup	21

	1.9.1 Electrochemical Cell	21
	1.10 Various electrochemical techniques	24
	1.10.1 Cyclic voltammetry (CV)	24
	1.10.2 Amperometry	27
	1.10.3 Chronoamperometry	28
	1.11 Sensor characterization	29
	1.11.1 Scanning electron microscopy (SEM)	29
	1.11.2 X-ray diffraction (XRD)	31
	1.12 Objectives of the present work	32
CHAPTER II	Literature review	
	2.1 Introduction	33
	2.2 Basic electrochemistry of graphene	35
	2.3 Direct electrochemistry of enzymes	36
	2.4 Graphene based electrodes for small bio-molecules	37
	2.4.1 Hydrogen peroxide (H ₂ O ₂)	37
	2.4.2 NADH	41
	2.4.3 Dopamine	43
	2.5 Graphene based electrochemical sensors	43
	2.5.1 Graphene based enzyme biosensors	43
	2.5.2 Graphene based electrochemical DNA biosensors	45
	2.5.3 Graphene based electrochemical sensors for heavy metal ions	45
	2.6 Attractive features and challenges of graphite pencil electrodes	47
	2.7 Future scope and outlook	48
CHAPTER III	Experimental	
	3.1 Materials	49
	3.2 Equipment	49
	3.3 preparation and polishing of pencil graphite electrodes (PGEs)	49
	3.4 Synthesis of SnO ₂ nano crystal	50
	3.5 Preparation of GO	50
	3.6 Modification of working electrode	51

	3.7 Standardization of the electrochemical System	51
CHAPTER IV	Results and Discussion	
	4.1 Electrochemical setup standardization	52
	4.2 Synthesis of nanoparticle and its physical characterization	55
	4.3 Sensor fabrication	56
	4.4 Electrocatalytic activity of blank HB, 2B, 3B and 4B PGEs	57
	4.5 Catalytic activity for H ₂ O ₂ reduction	59
	4.6 Conclusions	69
CHAPTER V	Conclusions and Recommendations	70
	References	

LIST OF TABLES

Table No	Description	Page
1.1	Density of aqueous solution of H ₂ O ₂ .	5
1.2	Properties of H ₂ O ₂ and its analogues (values marked * are extrapolated).	7
1.3	reduced product and its oxidation potential.	9
2.1	Some recent applications of PGE electrodes.	46
4.1	Electrochemical parameters obtained from voltammograms of fig 4.3.	53

LIST OF FIGURES

Figure No	Description	Page
1.1	Phase diagram of H ₂ O ₂ and water: Area above blue line is liquid. Dotted lines separate solid+ liquid phases from solid+ solid phases.	5
1.2	Structure and dimensions of H ₂ O ₂ in the gas phase.	6
1.3	Structure and dimensions of H ₂ O ₂ in the solid (crystalline) phase.	6
1.4	Mechanism of electrochemical sensor.	12
1.5	Structure of chitosan.	16
1.6	Schematic representation of the electrical double layer	18
1.7	Movement of charged particles in a potential field	19
1.8	Spontaneous movement of particles	20
1.9	Spontaneous movement of particles	21
1.10	Schematic Diagram of a voltammetric cell based on a three electrode system.	21
1.11	Gold disk working electrode	22
1.12	Ag/AgCl reference electrode	23
1.13	Platinum electrode	23
1.14	A potentiostat with circuit diagram of a three-electrode system.	24
1.15	Cyclic voltammetry input waveform.	25
1.16	Typical Cyclic Voltammogram response for a reversible redox couple.	25
1.17	(a) Current waveform for amperometric experiments. (b) A typical amperometric plot in stirred solution. Arrows indicate additions of the target analyte.	28
1.18	a) Excitation waveform b) current response output generated from the excitation waveform.	29
1.19	Different types of signals produced when high-energy electron impinges on a material.	30
1.20	Schematic diagram of a SEM	31
4.1	(a) CV of ferricyanide at 3B pencil graphite electrode were performed at concentration of 2mM of ferricyanide 0.1 M KNO ₃ as supporting electrolyte, different scan rate 20, 40, 60, 80, 100, 120, 140, 160mV/s.	52

Figure No	Description	Page
4.1	(b) The anodic and the cathodic peak heights as function of the square root of the scanning rate for pencil graphite electrode.	54
4.2	SEM micrographs of the surfaces of (A) bare pencil graphite electrode and (B) SnO ₂ -rGO/PGE.	56
4.3	Schematic diagram of stepwise fabrication of the H ₂ O ₂ sensor.	56
4.4	CV curves in HB PGEs (a) in the absence of H ₂ O ₂ and (b) in the presence of 0.1mM H ₂ O ₂ in 0.1M phosphate buffer solution (pH=7.4) containing at E _{app} = -1.0V (scan rate: 0.05 V/s).	57
4.5	CV curves in 2B PGC electrodes (a) in the absence of H ₂ O ₂ and (b) in the presence of 0.1mM H ₂ O ₂ in 0.1M phosphate buffer solution (pH=7.4) containing at E _{app} = -1.0V (scan rate: 0.05 V/s).	58
4.6	CV curves in 3B PGC electrodes (a) in the absence of H ₂ O ₂ and (b) in the presence of 0.1mM H ₂ O ₂ in 0.1M phosphate buffer solution (pH=7.4) containing at E _{app} = -1.0V (scan rate: 0.05 V/s).	59
4.7	CV curves in 4B PGC electrodes (a) in the absence of H ₂ O ₂ and (b) in the presence of 0.1mM H ₂ O ₂ in 0.1M phosphate buffer solution (pH=7.4) containing at E _{app} = -1.0V (scan rate: 0.05 V/s).	59
4.8	CVs of (a) blank 3B PGE and SnO ₂ -rGO/3B PGE in 0.1 M PBS (pH = 7.4) solution without and with 0.1 mM H ₂ O ₂ , potential scan rate 0.05 V s ⁻¹ .	61
4.9	CVs of rGO/3B PGE in 0.1 M PBS (pH = 7.4) solution without and with 0.1 mM H ₂ O ₂ , potential scan rate 0.05 V s ⁻¹ . (d) Reduced current on the square root of scan rate.	61
4.10	CVs of different scan rates (30 to 310 nV/s) of SnO ₂ -rGO/3B PGE in 0.1 M PBS (pH = 7.4) solution without and with 0.1 mM H ₂ O ₂ , potential scan rate 0.05 V s ⁻¹ .	62
4.11	Reduced current on the square root of scan rate.	62
4.12	(a) CVs of SnO ₂ -rGO/PGE in 0.1 M PBS buffer solution containing different concentrations of H ₂ O ₂ (from 0 to 1000 μM), potential scan rate 0.05 V s ⁻¹ .	63
4.12	(b) Dependence of reduction peak current on the concentration of H ₂ O ₂ .	64
4.13	Typical amperometric current response of the blank 3B PGEs upon the successive injection of H ₂ O ₂ with concentrations from 1mM to 7 mM into a stirred at E _{app} = -0.4V 0.1 M PBS pH 7.4.	65

Figure No	Description	Page
4.14	Typical amperometric current response of rGO modified 3B PGE upon the successive injection of H ₂ O ₂ with concentrations from 1mM to 7 mM into a stirred at E _{app} = -0.4V 0.1 M PBS pH 7.4	66
4.15	(a) Typical amperometric current response of SnO ₂ modified 3B PGE upon the successive injection of H ₂ O ₂ with concentrations from 1mM to 7 mM into a stirred at E _{app} = -0.4V 0.1 M PBS pH 7.4.	66
4.15	(b) Typical amperometric current response of the plot of concentration effect current density vs. the corresponding concentration of H ₂ O ₂ .	67
4.16	(a) Typical amperometric current response of the SnO ₂ -GO modified 3B PGEs upon the successive injection of H ₂ O ₂ with concentrations from 1mM to 8 mM into a stirred at E _{app} = -0.4V 0.1 M PBS pH 7.4.	68
4.16	(b) The plot of concentration effect current density vs. the corresponding concentration of H ₂ O ₂ .	68

Chapter I

Introduction

1.1. General

Electrochemistry deals with the conversion between chemical and electrical energy. This is achieved by two electrodes, an anode and a cathode, and an interconnecting electrolyte. At the electrode/electrolyte interfaces, chemical reactions take place, either driven by electrical energy or, on the contrary, yielding electrical energy. For such a process to function, the electrodes are to have high electronic conductivity while the electrolyte should have as low electronic conductivity as possible but instead high ionic conductivity [1]. Typically, electrochemical devices are layered thin-film structures, with the electrode electrolyte-electrode structure sandwiched. This design is used to minimize the energy losses in the system by shortening the distances between the components. Applications of electrochemistry bring a number of benefits. The most obvious advantage is utilized in devices world wide – the excellent energy storage capability. Secondary, i.e. rechargeable, batteries serve as a good illustration of the benefits electrochemistry can bring [2]. Not only can batteries store energy, they can also be recharged and used a large number of times, due to the possibility to make electrochemical systems reversible. It is also easy to control the rate of an electrochemical reaction, such as the output current of a battery. However, many electrochemical systems, such as batteries, are temperature dependent; unwanted side reactions develop at higher temperatures [3].

Today, electroanalytical chemistry can play a vital role in nanotechnologies. Nanotechnologies are now poised to revolution the electronic, chemical and biotechnology industries and biomedical. There are many interesting areas in nanotechnology [4, 5]. One of the most important aspects in this field is the preparation and development of nonmaterial's, such as nanoparticles [6–10]. Nanoparticles can be made with different materials as small as 1 nm. Nanoparticles are useful in biochemical analysis, such as in sensors and biomarkers. In the past twenty years, the development of studies on chemical sensors and biosensors was very rapid [11].

Electrochemical sensors continues unabated today, stimulated by the wide range of potential applications. Their impact is most clearly illustrated in the widespread use of electrochemical sensors seen in daily life, where they continue to meet the expanding need for rapid, simple and economic methods of determination of numerous analytes.

Hydrogen peroxide (H_2O_2) is one of the most common reactive oxygen species (ROS), and its concentration is an active area of research due to potential biological, industrial, and environmental applications [12, 13]. Biologically, H_2O_2 plays a significant role as a signaling and regulating molecule within cells and between cells [14, 15]. In addition, the concentration of H_2O_2 is a weighty biological parameter because H_2O_2 is a reactive oxygen species (ROS), which is a product of metabolism in the human body [16] and results in oxidative stress [17,18]. High levels of oxidative stress caused by ROS may damage DNA and contribute to cancer [19]. Quantitative analyses of H_2O_2 are indicative of oxidative stress and easily determined in the intact human organism [20]. Moreover, studies of H_2O_2 concentration are considered key solutions for neurodegenerative disease, cancer, etc. [21, 22]. Accordingly, an efficient detection method for simple, exact, and expeditious sensing of H_2O_2 has been sought. Microfluidics offers a convenient and immediate sensing platform to detect specific biomolecules [23]. Over the past 2 decades, a number of microfluidic systems have shown potential to meet requirements including small sample volume, low cost, fast sample analysis, and improved reaction reliability and reproducibility [24, 25]. Making use of these properties of microfluidics, numerous biosensors combined with microfluidics have been developed to improve the overall performance of the sensing system, particularly electrochemical biosensors integrated in microfluidics, which are used in point-of-care diagnostics [26,27].

Electrochemical biosensors have attracted much attention due to their inexpensive analysis, simple manipulations, high sensitivity and selectivity, and ease of portability for miniaturized healthcare sensors [28]. Therefore, electrochemical detection has been widely applied for on chip and real-time monitoring systems [29]. Although electrochemical sensors for quantification of H_2O_2 have virtues such as convenient operation, speed, sensitivity, cost effectiveness, and ease of integration onto an on-chip system, the electrochemical detection of H_2O_2 has limits associated with high over potential and slow electron transfer [30]. To improve the sensitivity of the electrochemical sensors, the modification of noble metal nanoparticles (NPs) onto the electrode could be used to

decrease over potential and increase electrode kinetics [31]. NPs are beneficial for the development of biosensing techniques due to high surface areas, strong stability, limited aggregation, and high electrocatalytic activity.

Moreover, the electrochemical deposition of metal NPs into the microchannel can accurately control the position of nanostructures, maximize the stability of the electrode, and ensure that miniaturized electrochemical sensors with NPs are more specific and highly sensitive for biomolecular diagnostics [32, 33]. So it is very important to detect of H₂O₂ fluctuation.

Electrochemical screening techniques are the most popular compare to other central laboratory based techniques such as spectrophotometric [34] or chromatographic [35] techniques. It is due to the growing demand for development of in situ, portable, cost effective methodology, where electrochemical techniques have proven advantages for such applications. However, challenges are attributed to such developments are selectivity, sensitivity, response time, stability, biocompatibility and reproducibility. Trends for researchers and manufacturers working with the micro and nanostructured materials as sensing platform is growing popularity due to the higher sensitivity and lower noise, can be used for in situ technology, as well as more suitable towards biocompatibility, improve response time, stability and reproducibility.

In this work, graphene oxide and stannic oxide + chitosan modified pencil graphite electrode (GO-SnO₂/PGE) electrode was prepared for the detection of H₂O₂. The electrochemical properties of this sensor were investigated. This sensor exhibited rapid response, low detection limit and broad linear range.

1.2 Description of H₂O₂

Hydrogen peroxide is a chemical compound with the formula H₂O₂. In its pure form, it is a colorless liquid, slightly more viscous than water; however, for safety reasons it is normally used as a solution. Hydrogen peroxide is the simplest peroxide (a compound with an oxygen–oxygen single bond) and finds use as a weak oxidizer, bleaching agent and disinfectant. Concentrated hydrogen peroxide, or “high- test peroxide”, is a reactive Oxygen species and has been used as a propellant in rocketry.

Hydrogen peroxide is often described as being "water but with one more oxygen atom", a description that can give the incorrect impression of significant chemical similarity between the two compounds. While they have a similar melting point and appearance, pure hydrogen peroxide will explode if heated to boiling, will cause serious contact burns to the skin and can set materials alight on contact. For these reasons it is usually handled as a dilute solution (household grades are typically 3–6% in the U.S. and somewhat higher in Europe). Its chemistry is dominated by the nature of its unstable peroxide bond.

1.3. Structure and properties of H₂O₂

1.3.1. Properties

The boiling point of H₂O₂ has been extrapolated as being 150.2 °C, approximately 50 °C higher than water. In practice hydrogen peroxide will undergo potentially explosive thermal decomposition if heated to this temperature. It may be safely distilled at lower temperatures under reduced pressure [36].

1.3.2. Aqueous solutions

In aqueous solutions hydrogen peroxide differs from the pure material due to the effects of hydrogen bonding between water and hydrogen peroxide molecules. Hydrogen peroxide and water form a eutectic mixture, exhibiting- freezing point depression; pure water has a melting point of 0 °C and pure hydrogen peroxide of –0.43 °C, but a 50% (by volume) solution of the two freezes at –51 °C. The boiling point of the same mixtures is also depressed in relation with the mean of both boiling points (125.1 °C). It occurs at 114 °C. This boiling point is 14 °C greater than that of pure water and 36.2 °C less than that of pure hydrogen peroxide [37].

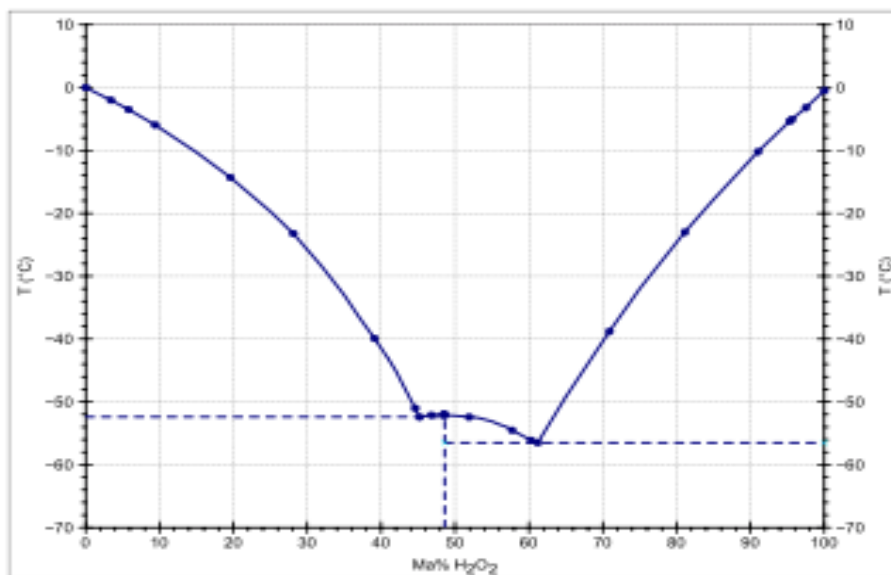


Figure 1.1 : Phase diagram of H₂O₂ and water: Area above blue line is liquid. Dotted lines separate solid+ liquid phases from solid+ solid phases.

Table 1.1 : Density of aqueous solution of H₂O₂

H ₂ O ₂ (w/w)	Density (g/cm ³)	Temperature (°C)
3%	1.00	15
27%	1.10	20
35%	1.13	20
50%	1.20	20
70%	1.29	20
75%	1.33	20
96%	1.42	20
98%	1.43	20
100%	1.45	20

1.3.3. Structure of H₂O₂

Hydrogen peroxide (H₂O₂) is a nonplanar molecule with (twisted) C₂ symmetry. Although the O–O bond is a single bond, the molecule has a relatively high rotational barrier of 2460 cm⁻¹ (29.45 kJ/mol; for comparison, the rotational barrier for ethane is 12.5 kJ/mol). The increased barrier is ascribed to repulsion between the lone pairs of the adjacent oxygen atoms and results in hydrogen peroxide displaying atropisomerism.

The molecular structures of gaseous and crystalline H₂O₂ are significantly different. This difference is attributed to the effects of hydrogen bonding, which is absent in the gaseous state [38]. Crystals of H₂O₂ are tetragonal with the space group *D*4₄*P*₄₁₂₁ [39].

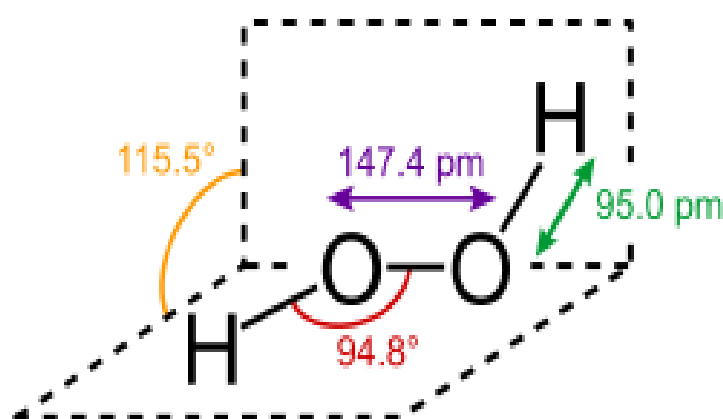


Figure 1.2 : Structure and dimensions of H₂O₂ in the gas phase

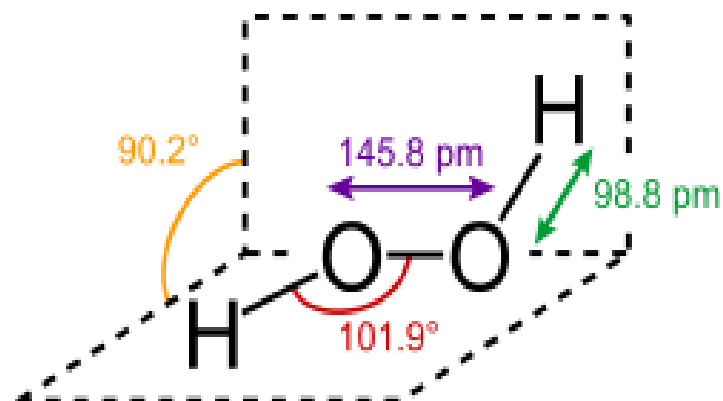


Figure 1.3 : Structure and dimensions of H₂O₂ in the solid (crystalline) phase

Table 1.2 : Properties of H₂O₂ and its analogues (values marked * are extrapolated)

Name	Formula	Molar mass(g/mol)	T _M (°C)	T _B (°C)
Hydrogen peroxide	HOOH	34.01	-0.43	150.2*
Water	HOH	18.02	0.00	99.98
Hydrogen disulfide	HSSH	66.15	-89.6	70.7
Hydrazine	H ₂ NNH ₂	32.05	2	114
Hydroxylamine	NH ₂ OH	33.03	33	58*
Diphosphane	H ₂ PPH ₂	65.98	-99	63.5*

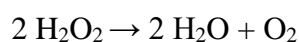
1.3.4. Comparison with analogues

Hydrogen peroxide has several structural analogues with H-X-X-H bonding arrangements (water also shown for comparison). It has the highest (theoretical) boiling point of this series (X = O, N, S). Its melting point is also fairly high, being comparable to that of hydrogen and water, with only hydroxylamine crystallising significantly more readily, indicative of particularly strong hydrogen bonding. Diphosphane and hydrogen disulfide exhibit only weak hydrogen bonding and have little chemical similarity to hydrogen peroxide. All of these analogues are thermodynamically unstable. Structurally, the analogues all adopt similar skewed structures, due to repulsion between adjacent lone pairs.

1.4. Reactions of H₂O₂

1.4.1. Decomposition

Hydrogen peroxide is thermodynamically unstable and decomposes to form water and oxygen with a ΔH_o of -98.2 kJ/mol and a ΔS of 70.5 J/ (mol·K):



The rate of decomposition increases with rising temperature, concentration and pH, with cool, dilute, acidic solutions showing the best stability. Decomposition is catalysed by various compounds, including most transition metals and their compounds (e.g. manganese dioxide, silver, and platinum) [40]. Certain metal ions, such as Fe^{2+} or Ti^{3+} , can cause the decomposition to take a different path, with free radicals such as $(\text{HO}\cdot)$ and $(\text{HOO}\cdot)$ being formed. Non-metallic catalysts include potassium iodide, which reacts particularly rapidly and forms the basis of the elephant toothpaste experiment. Hydrogen peroxide can also be decomposed biologically by the enzyme catalase. The decomposition of hydrogen peroxide liberates oxygen and heat; this can be dangerous, as spilling high-concentration hydrogen peroxide on a flammable substance can cause an immediate fire.

1.4.2. Redox reactions

Hydrogen peroxide exhibits oxidizing and reducing properties, depending on pH. In acidic solutions, H_2O_2 is one of the most powerful oxidizers known—stronger than chlorine, chlorine dioxide, and potassium permanganate. Also, through catalysis, H_2O_2 can be converted into hydroxyl radicals $(\cdot\text{OH})$, which are highly reactive.

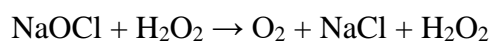
Table 1.3 : reduced product and its oxidation potential

Oxidant/reduced product	Oxidation potential, V
fluorine/hydrogen fluoride	3.0
ozone/oxygen	2.1
hydrogen peroxide/water	1.8
potassium permanganate/manganese dioxide	1.7
chlorine dioxide/ HClO	1.5
chlorine/chloride	1.4

In acidic solutions Fe^{2+} is oxidized to Fe^{3+} (hydrogen peroxide acting as an oxidizing agent):

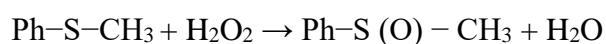
$2 \text{Fe}^{2+} (\text{aq}) + \text{H}_2\text{O}_2 + 2 \text{H}^+ (\text{aq}) \rightarrow 2 \text{Fe}^{3+} (\text{aq}) + 2 \text{H}_2\text{O} (\text{l})$ and sulfite (SO_3^{2-}) is oxidized to sulfate (SO_4^{2-}). However, potassium permanganate is reduced to Mn^{2+} by acidic H_2O_2 . Under alkaline conditions, however, some of these reactions reverse; for example, Mn^{2+} is oxidized to Mn^{4+} (as MnO_2).

In basic solution, hydrogen peroxide can reduce a variety of inorganic ions. When it acts as a reducing agent, oxygen gas is also produced. For example, hydrogen peroxide will reduce sodium hypochlorite and potassium permanganate, which is a convenient method for preparing oxygen in the laboratory:



1.4.3. Reactons with Organic Compounds

Hydrogen peroxide is frequently used as an oxidizing agent. Illustrative is oxidation of thioethers to sulfoxides: [41] [42]



Alkaline hydrogen peroxide is used for epoxidation of electron-deficient alkenes such as acrylic acid derivatives, and for the oxidation of alkylboranes to alcohols, the second step of hydroboration-oxidation. It is also the principal reagent in the Dakin oxidation process.

1.5. Precursor to other peroxide compounds

Hydrogen peroxide is a weak acid, forming hydroperoxide or peroxide salts with many metals. It also converts metal oxides into the corresponding peroxides. For example, upon

treatment with hydrogen peroxide, chromic acid ($\text{CrO}_3 + \text{H}_2\text{SO}_4$) forms an unstable blue peroxide $\text{CrO}(\text{O}_2)_2$.

This kind of reaction is used industrially to produce peroxyanions. For example, reaction with borax leads to sodium perborate, a bleach used in laundry detergents:



H_2O_2 converts carboxylic acids (RCO_2H) into peroxy acids ($\text{RC}(\text{O})\text{O}_2\text{H}$), which are themselves used as oxidizing agents. Hydrogen peroxide reacts with acetone to form acetone peroxide and with ozone to form trioxidane. Hydrogen peroxide forms stable adducts with urea (hydrogen peroxide - urea), sodium carbonate (sodium percarbonate) and other compounds [43]. An acid-base adduct with triphenylphosphine oxide is a useful "carrier" for H_2O_2 in some reactions.

The peroxide anion is a stronger nucleophile than hydroxide and displaces hydroxyl from oxyanions e.g. forming perborates and percarbonates. Sodium perborate and sodium percarbonate are important consumer and industrial bleaching agents; they stabilize hydrogen peroxide and limit side reactions (e.g. reduction and decomposition note below). The peroxide anion forms an adduct with urea, hydrogen peroxide–urea.

Hydrogen peroxide is both an oxidizing agent and reducing agent. The oxidation of hydrogen peroxide by sodium hypochlorite yields singlet oxygen. The net reaction of a ferric ion with hydrogen peroxide is a ferrous ion and oxygen. This proceeds via single electron oxidation and hydroxyl radicals. This is used in some organic chemistry oxidations, e.g. in the Fenton's reagent. Only catalytic quantities of iron ion is needed since peroxide also oxidizes ferrous to ferric ion. The net reaction of hydrogen peroxide and permanganate or manganese dioxide is manganous ion; however, until the peroxide is spent some manganous ions are reoxidized to make the reaction catalytic. This forms the basis for common monopropellant rockets.

1.6. Electrochemical sensors

Electrochemical sensors are the devices, which are composed of an active sensing material with a signal transducer. The role of these two important components in sensors is to

transmit the signal without any amplification from a selective compound or from a change in a reaction. These devices produce any one of the signals as electrical, thermal or optical output signals which could be converted into digital signals for further processing. One of the ways of classifying sensors is done based on these output signals. Among these, electrochemical sensors have more advantage over the others because; in these, the electrodes can sense the materials which are present within the host without doing any damage to the host system. On the other hand, sensors can be broadly classified into two categories as chemical sensors and biosensors. The biosensors can be defined in terms of sensing aspects, where these sensors can sense biochemical compounds such as biological proteins, nucleotides and even tissues [43].

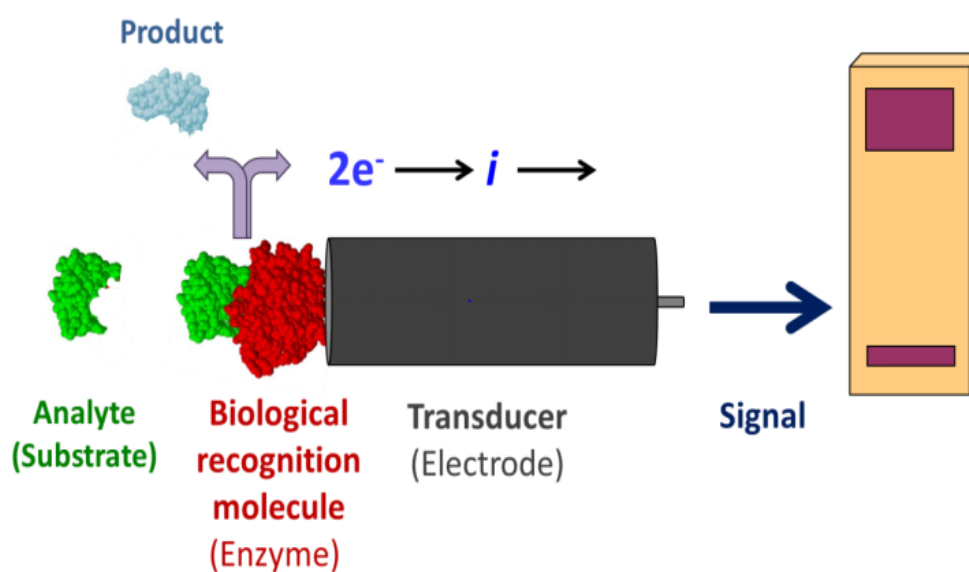


Fig. 1.4: Mechanism of electrochemical sensor.

Depending on the exact mode of signal transduction, electrochemical sensors can use a range of modes of detection such as potentiometric, voltammetric and conductimetric. Each principle requires a specific design of the electrochemical cell. Potentiometric sensors are very attractive for field operations because of their high selectivity, simplicity and low cost. They are, however, less sensitive and often slower than their voltammetric counterparts. Examples of transduction techniques include:

Potentiometric – The measurement of the potential at zero current. The potential is proportional to the logarithm of the concentration of the substance being determined.

Voltammetric – Increasing or decrease the potential that is applied to a cell until the oxidation or reduction of the analyte occurs. This generates a rise in current that is proportional to the concentration of the electroactive potential. Once the desired stable oxidation/reduction potential is known, stepping the potential directly to that value and observing the current is known as amperometry.

Conductiometric – Observing changes in electrical conductivity of the solution [44].

The selection and development of an active material is a challenge. The active sensing materials may be of any kind as whichever acts as a catalyst for sensing a particular analyte or a set of analytes. The recent development in the nanotechnology has paved the way for large number of new materials and devices of desirable properties which have useful functions for numerous electrochemical sensor and biosensor applications.

Basically by creating nanostructure, it is possible to control the fundamental properties of materials even without changing their chemical composition. In this way the attractive world of low dimensional systems, together with the current tendencies on the fabrication of functional nanostructured arrays could play a key role in the new trends of nanotechnology [45, 46, 47].

Further, the nanostructures can be used for both efficient transport of electrons and optical excitation, and these two factors make them critical to the function and integration of nanoscale devices [48-50]. In fact, nano systems are the smallest dimension structures that can be used for efficient transport of electrons and are thus critical to the function and integration of these nanoscale devices.

1.7. Chemically modified electrodes

Chemically modified electrodes (CMEs) comprise a relatively modern approach to electrode systems a wide spectrum of basic electrochemical investigations, including the relationship of heterogeneous electron transfer and chemical reactivity to electrode surface chemistry, electrostatic phenomena at electrode surfaces, and electron and ionic transport phenomena in polymers, and the design of electrochemical devices and systems for

applications in chemical sensing, energy conversion and storage, molecular electronics, electrochromic displays, corrosion protection, and electro-organic syntheses. Compared with other electrode concepts in electrochemistry, the distinguishing feature of a CME is that a generally quite thin film (from a molecular monolayer to perhaps a few micrometers-thick multilayer) of a selected chemical is bonded to or coated on the electrode surface to endow the electrode with the chemical, electrochemical, optical, electrical, transport, and other desirable properties of the film in a rational, chemically designed manner [51].

The range of electrode surface properties includes, but is more diverse than, that of ion-selective electrodes (ISEs) which also involve, in their highest forms, rational design of the phase-boundary, partition and transport properties of membranes on or between electrodes. While CMEs can operate both amperometrically (or voltammetrically) and potentiometrically, they are generally used amperometrically, a faradaic (charge transfer) reaction being the basis of experimental measurement or study, whereas ISEs are generally used in potentiometric formats where a phase-boundary potential (interfacial potential difference) is the measured quantity [52]. Gas-sensing electrodes (e.g., for CO₂, NH₃, NO_x) are also potentiometrically based [53] although the oxygen electrode, which functions amperometrically, is an exception [54]. Chemically sensitive field effect transistors (CHEMFETs) are basically non-faradaic electrode systems in which electric field variations in the semiconductor gate region control the magnitude of the source drain current [55]. Enzyme-based electrodes detect the product(s) of a reaction between an immobilized enzyme layer and a reaction substrate in many ways, including both amperometric and potentiometric means. The distinction between CMEs and amperometric enzyme-modified electrodes is thus very narrow, the latter being based on a natural biological catalyst, but also with a rational (bio) molecular electrode design goal in mind.

1.7.1. General methods of modification of electrodes

The concept of chemically modified electrodes (CMEs) is one of the exciting developments in the field of electroanalytical chemistry. Many different strategies have been employed for the modification of the electrode surface. The motivations behind the modifications of the electrode surface are: (i) improved electrocatalysis, (ii) freedom from

surface fouling and (iii) prevention of undesirable reactions competing kinetically with the desired electrode process [56]. The increasing demand for it has led to the development of a rapid, simple and non-separation method for the simultaneous determination of isomers where the CMEs have emerged as an efficient and versatile approach, and have attracted considerable attention over the past decades due to its advantages in terms of reduced costs, automatic and fast analysis, high sensitivity and selectivity [57-61]. There are numerous techniques that may be used to modify electrode surfaces. Among various CMEs, polymer-modified electrodes (PMEs) are promising approach to determination. Some modification processes are-

Covalent Bonding: This method employs a linking agent (e.g. an organosilane) to covalently attach one of several monomolecular layers of the chemical modifier to the electrode surface [59].

Drop-Dry Coating (or solvent evaporation): A few drops of the polymer, modifier or catalyst solution are dropped onto the electrode surface and left to stand to allow the solvent to dry out [60].

Dry-Dip Coating: The electrode is immersed in a solution of the polymer, modifier or catalyst for a period sufficient for spontaneous film formation to occur by adsorption. The electrode is then removed from solution and the solvent is allowed to dry out [57].

Composite: The chemical modifier is simply mixed with an electrode matrix material, as in the case of an electron-transfer mediator (electrocatalyst) combined with the carbon particles (plus binder) of a carbon paste electrode. Alternatively, intercalation matrices such as certain Langmuir-Blodgett films, zeolites, clays and molecular sieves can be used to contain the modifier [61].

Spin-Coating (or Spin-Casting): it is also called spin casting, a droplet of a dilute solution of the polymer is applied to the surface of a rotating electrode. Excess solution is spun off the surface and the remaining thin polymer film is allowed to dry. Multiple layers are applied in the same way until the desired thickness is obtained. This procedure typically produces pinhole-free thin films for example; oxide xerogel film electrodes prepared by spin-coating a viscous gel on an indium oxide substrate [57].

Electro deposition: In this technique the electrode is immersed in a concentrated solution ($\sim 10^{-3}$ molL⁻¹) of the polymer, modifier or catalyst followed by repetitive voltammetry scans. The first and second scans are similar, subsequent scans decrease with the peak current. For example, electrochemical deposition of poly (o-toluidine) on activated carbon fibre [61].

Electropolymerisation: A solution of monomer is oxidized or reduced to an activated form that polymerizes to form a polymer film directly on the electrode surface. This procedure results in few pinholes since polymerization would be accentuated at exposed (pinhole) sites at the electrode surface. Unless the polymer film itself is redox active, electrode passivation occurs and further film growth is prevented.

In this technique the electrode is immersed in a polymer, modifier or catalyst solution and layers of the electropolymerized material builds on the electrode surface. Generally, the peak current increases with each voltammetry scan such that there is a noticeable difference between the first and final scans indicating the presence of the polymerized material. For example, electropolymerization of aniline on platinum electrode perturbations.

Chitosan: Chitosan is a derivative of chitin, which is one of the world's most plentiful organic resources and is derived from the shells of crustaceans. It is a linear polyaminosaccharaide composed of randomly distributed β -(1,4)-linked D-glucosamine and N-acetyl-D-glucosamine groups. Due to its structure, chitosan possesses good adhesion and cheap properties, therefore it has been used as an immobilization matrix. Although it has poor electrical conductivity, but it usually has been combined with carbon nanotubes, redox mediator and metal nanoparticles [62].

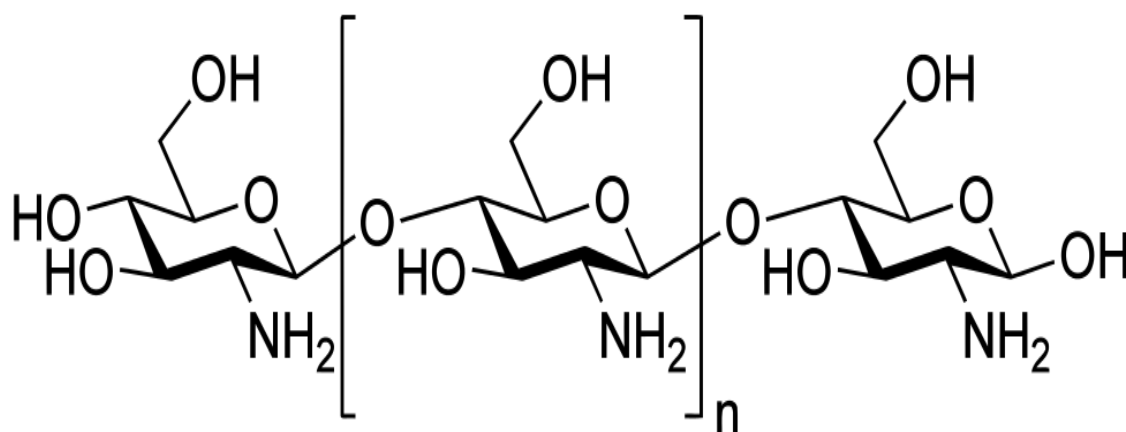


Fig 1.5: Structure of chitosan.

Chitosan is soluble in aqueous acidic media at $\text{pH} < 6.5$. When dissolved, it bears a high positive charge on its amino groups. Chitosan has gel-forming properties as a result of its ability to adhere to negatively charged surfaces and aggregate polyanionic compounds.

1.8. Fundamentals of electrochemistry

Faradic currents: Faradic current is the sum of all type of currents that are generated due to the electrochemical reaction of analyte in the cell. It is called faradic because it obeys faradays laws of electrolysis. Examples of faradic currents include diffusion current which is the term of interest in polarographic analysis. Kinetic currents are part of the faradic current where it should be clear that reactions should be rapid but of lower rate than the diffusion of the analyte. Kinetic currents are sensitive to changes in temperature with just small contribution to the faradic current. Most of the faradic current thus originates from the diffusion current.

Non Faradic Currents: These do not obey faraday's laws of electrolysis and are thus of no analytical value. The most important contribution to non-faradic currents originates from what is called capacitive current. This capacitive current results from the double layer which is formed between the charged mercury drop and the counter ions at the solution interface. Another contribution comes from migration current which results from electrostatic attraction of analyte ions by the oppositely charged mercury drop. Addition of supporting electrolyte of enough concentration will make this term close to zero.

Charging currents and the Electrical Double Layer: The application of a potential to the electrode surface causes ions near the electrode surface to migrate towards or away from the electrode depending on the respective charge of the electrode and the ions. This forms an electrical double layer, comprised of the electrical charge at the surface of the electrode and the charge of the ions in the solution near the electrode. This double layer leads to the generation of a non-faradaic charging current. Whenever a charged solid surface is placed in any solution, the ions, carrying charge opposite to that carried by the surface, cluster around the solid surface. These sheet of ionic charge adjacent to the charged solid surface and the charged surface constitute a double layer. The electrical double layer is an array of charged particles and orientated dipoles. It is composed of two layers; the layer closest to the electrode is known as the inner Helmholtz plane (IHP) and the outer Helmholtz plane (OHP) (Fig 1.6). The planes were discovered by Hermann von Helmholtz in 1853. The IHP is composed of solvent molecules and specifically adsorbed ions, whilst the OHP represents the imagined outer layer closest to the electrode that passes through the centre of solvated ions, but is separated by the molecules at the IHP. These layers are both held at the surface of the electrode. The behavior of the interface between the electrode and the solution is similar to that of a capacitor.

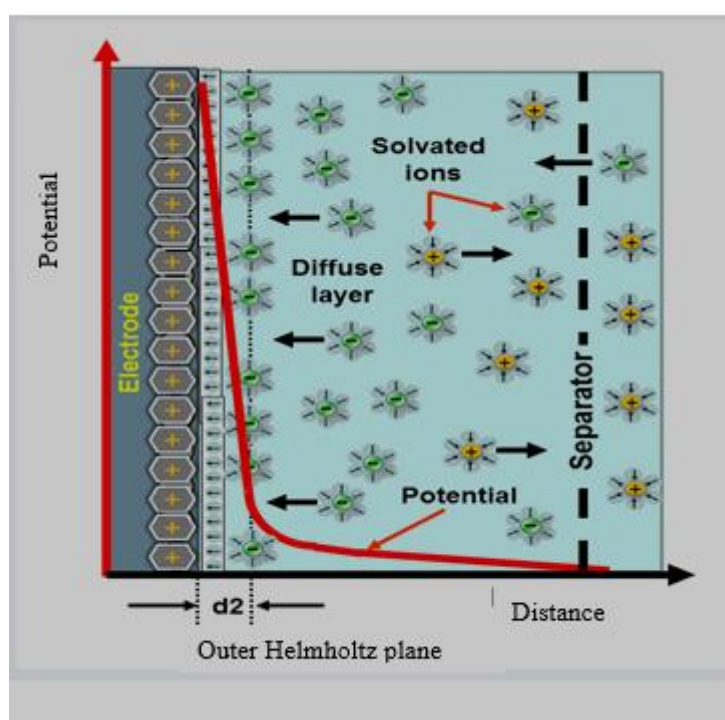


Figure 1.6: Schematic representation of the electrical double layer [63].

Beyond the double layer, is a diffuse layer of scattered ions that extends into the bulk solution. These ions are ordered relative to the columbic forces acting upon them and the random motion of the solution by thermal motion. The balance of the electrostatic forces on ions at the surface of the electrode, which are repelled or attracted dependent on their charge, is counterbalanced by the random motion of the diffuse layer. This causes a non-uniform distribution of ions near the electrode surface. As a result, the field strength of the potential applied to the electrode diminishes rapidly, thereby causing the double layer to be extremely thin at 10 – 20 nanometers in thickness. It is also essential to use a high electrolyte concentration, typically a 100 fold greater than that of the analyte, as this concentrates the charge at the Helmholtz planes, therefore ensuring that diffusion is the dominant mechanism for mass transport [64].

Mass transfer process in voltammetry: The movement of the electro-active substance through solution is called mass transfer at the electrode surface. In electrochemical systems, three modes of mass transport are generally considered which a substance may be carried to the electrode surface from bulk solution including diffusion, convection and migration. Any of these or more than one might be operating in a given experiment which is depended on the experimental conditions.

In general, there are three types of mass transfer processes:

Migration: Migration is the movement of ions through a solution as a result of electrostatic attraction between the ions and the electrodes. It is the primary cause of mass transfer in the bulk of the solution in a cell. This motion of charged particle through solution, induced by the charges on the electrodes is called migration. This charge movement constitutes a current. This current is called migration current. The larger the number of different kinds of ions in a given solution, the smaller is the fraction of the total charge that is carried by a particular species. Electrolysis is carried out with a large excess of inert electrolyte in the solution so the current of electrons through the external circuit can be balanced by the passage of ions through the solution between the electrodes, and a minimal amount of the electroactive species will be transported by migration. Migration is the movement of charged species due to a potential gradient. In voltammetric experiments, migration is undesirable but can be eliminated by the addition of a large excess of

supporting electrolytes in the electrolysis solution. The effect of migration is applied zero by a factor of fifty to hundred ions excess of an inert supporting electrolyte.

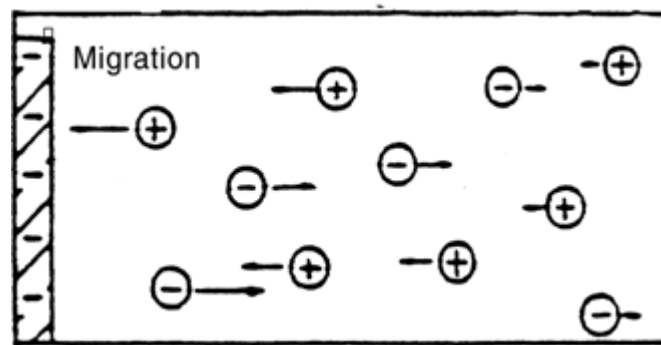


Figure 1.7: Movement of charged particles in a potential field [64].

Diffusion: Diffusion refers to the process by which molecules intermingle as a result of their kinetic energy of random motion. Whereas a concentration difference between two regions of a solution, ions or molecules move from the more concentrated region to the dilute and leads to a disappearance of the concentration difference.

The one kind of mode of mass transfer is diffusion to an electrode surface in an electrochemical cell. The rate of diffusion is directly proportional to the concentration difference. When the potential is applied, the cations are reduced at the electrode surface and the concentration is decreased at the surface film. Hence a concentration gradient is produced. Finally, the result is that the rates of diffusion current become larger.

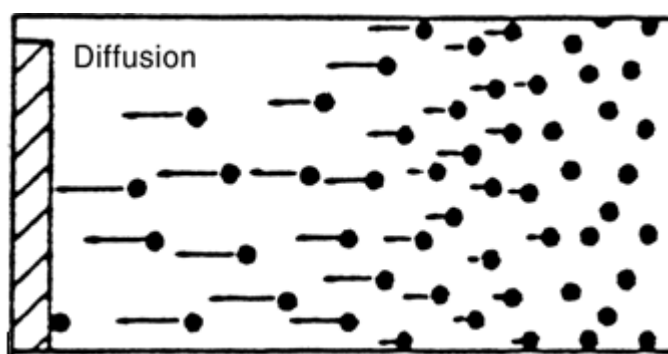


Figure 1.8: Spontaneous movement of particles [64].

Convection: By mechanical way reactants can also be transferred to or from an electrode. Thus forced convection is the movement of a substance through solution by stirring or

agitation. This will tend to decrease the thickness of the diffuse layer at an electrode surface and thus decrease concentration polarization. Natural convection resulting from temperature or density differences also contributes to the transport of species to and from the electrode. At the same time a type of current is produced. This current is called convection current. Removing the stirring and heating can eliminate this current. Convection is a far more efficient means of mass transport than diffusion.

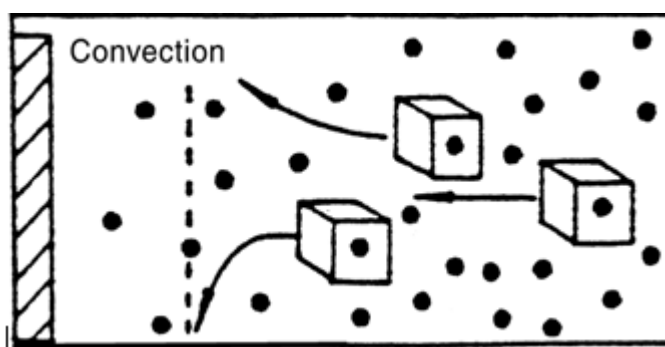


Figure 1.9 : Spontaneous movement of particles [65].

1.9. Electrochemical setup

1.9.1 Electrochemical cell

An electrochemical cell is a device that capable of either generating electrical energy from chemical reaction or facilitating chemical reactions through the introduction of electrical energy. An electrochemical cell consists two half-cells. Each half-cell consists of an electrode and an analyte. An electrode is an electrical conductor used to make contact with a non-metallic part of a circuit (eg. a semiconductor, an electrolyte or a vacuum).An electrolyte is a substance that ionizes when dissolved in suitable ionizing solvent. This can conduct electricity in solution. This can be organic, inorganic or organometallic compounds.

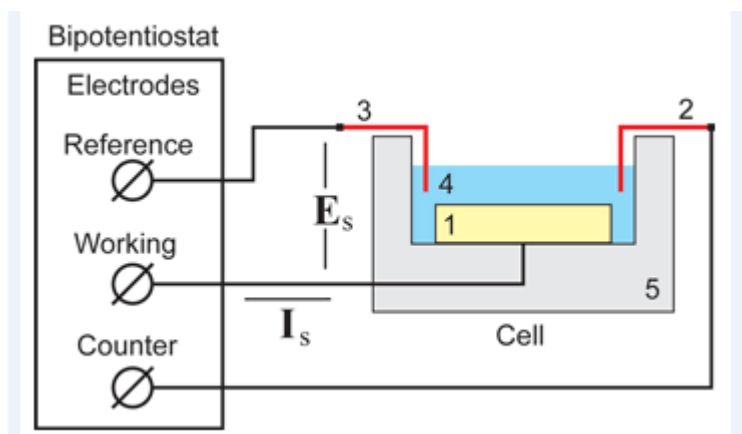


Figure 1.10: Schematic Diagram of a voltammetric cell based on a three electrode system. CE: counter electrode, WE: Working electrode, RE: Reference electrode. This is an example of a three electrode cell [Google].

Electrodes: An electrode is an electrical conductor used to make contact with a nonmetallic part of a circuit (e.g. a semiconductor, an electrolyte or a vacuum). Types of electrode

- ❖ Working electrode
- ❖ Reference electrode
- ❖ Counter electrode

Working Electrode (WE): Working electrode (WE) is one which electrochemical reaction occurs. The working electrode makes contact with the analyte and transfer charge to and from the analyte. The working electrode must be made of a material that is stable in the electrolyte medium utilized during the experiment, e.g.: carbon. This is to ensure that the electrode does not corrode or become fouled, thereby altering the surface area, and to prevent other compounds reducing in the potential range of interest. Working electrodes should have high surface reproducibility with a uniform distribution of potential across the surface to prevent IR drop. The background current within the potential region of interest should be low. The cost, availability and toxicity of the material should also be considered.



Figure 1.11: gold disk working electrode. [Wikipedia]

Reference Electrode: A reference electrode acts as a half-cell which has a stable and accurately maintained potential which is used as a reference for the measurement of voltage applied by the counter electrode (CE). It is potentiometric and thus has zero current flowing through it. The potentiostat compensates if a difference in voltage is detected between the AE and WE and adjusts the output accordingly until the difference is zero, this action is known as feedback [66]. An example of a commonly used reference electrode is the silver-silver chloride (Ag/AgCl). For applications such as chrono amperometry where small currents are flowing for short time periods, two electrode systems may be used, where the counter electrode assumes the role of RE and WE. Since current flowing through the reference electrode may alter its stability over time, three electrode systems with a counter electrode are often utilized in experimental situations, and for square-wave voltammetric applications over prolonged time periods.



Figure 1.12: Ag/AgCl reference electrode

Counter Electrode: It is also called auxiliary electrode, is used to balance the electric current that is expected to flow through the working electrode. The CE is composed of an inert material such as carbon or platinum.



Figure 1.13: Platinum electrode [67].

Potentiostat: The instrument used to control the potential difference applied across the electrochemical cell is called a potentiostat. A potentiostat adjusts the voltage difference between the anode and the cathode in order to maintain a constant working electrode potential. A potential is applied to the working electrode, resulting in a flow of charge towards the counter electrode. A potential drop (iR) is caused by the electrolyte conductivity, the distance between the electrodes, the magnitude of the current and resistance across the electrode material. If the iR drop is uncompensated, the reaction will no longer operate at the desired potential, and the reaction may cease. The reference electrode monitors the potential at the working electrode and feeds the value back to the opamp. If a difference in potential is observed between the RE and WE, the potential applied to the CE is altered to compensate. A second op-amp is used as a current-voltage converter to measure the flow of current, with a resistor used to output the voltage per unit current.

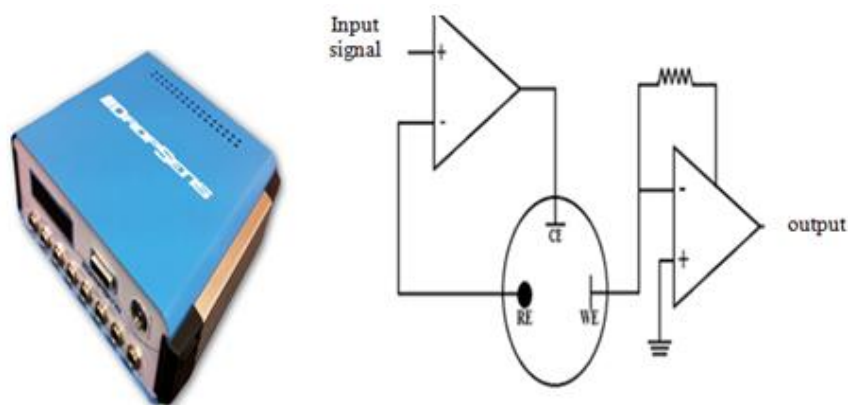


Figure 1.14: A potentiostat with circuit diagram of a three-electrode system.

1.10 Various electrochemical techniques

1.10.1 Cyclic voltammetry (CV)

Cyclic voltammetry is a commonly used and versatile potentiodynamic electroanalytical technique used to study redox systems, the reversibility of the reaction, the stoichiometry of a system and the diffusion coefficient of an analyte. These can be used to determine the electrochemical characteristics and identity of an unknown compound.

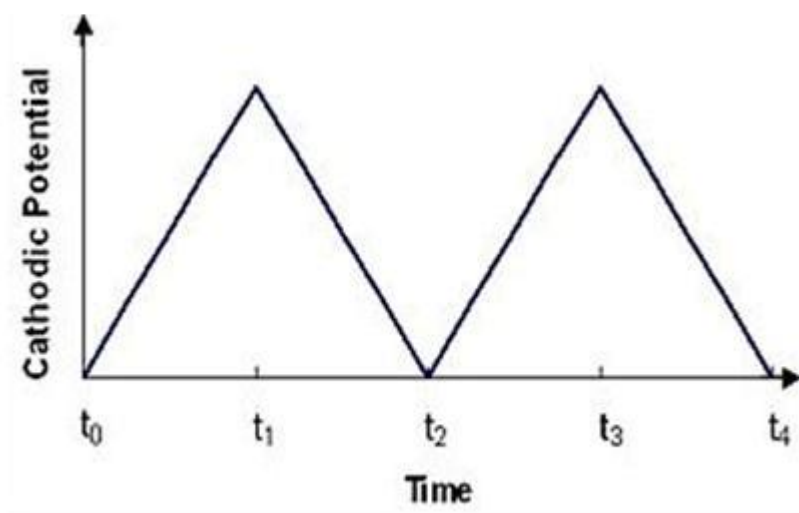


Figure 1.15: Cyclic voltammetry input waveform.

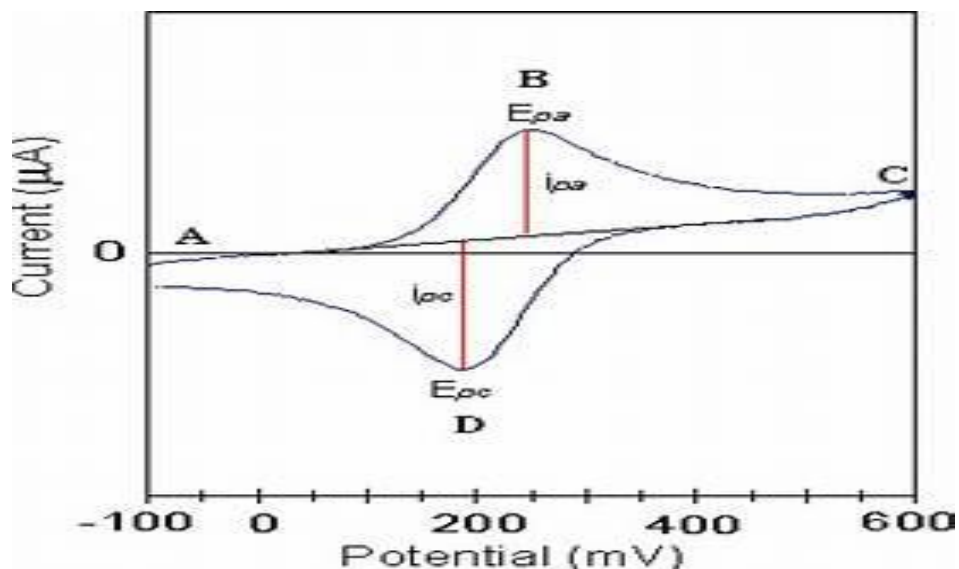


Figure 1.16: Typical Cyclic Voltammogram response for a reversible redox couple.

Cyclic voltammograms are characterized by six important parameters.

- The cathodic (E_{pc}) and anodic (E_{pa}) peak potentials
- The cathodic (i_{pc}) and anodic (i_{pa}) peak currents
- The cathodic half-peak potential ($E_{p/2}$)
- The half wave potential ($E_{1/2}$)

Cyclic voltammetry linearly applies a triangular potential ramp to the working electrode at a defined scan rate until it has reached a set switching potential as shown in Fig 1.7. Once the switching potential on the triangular excitation potential ramp is reached, it begins a scan in the reverse direction. During the potential sweep, the current is measured resulting from the potential applied. The resulting plot of current vs. potential is known as a cyclic voltammogram, as illustrated in Fig. 1.16.

The two peak currents (i_{pc}/i_{pa}) and two peak potentials (E_{pc}/E_{pa}) form the basis for the analysis of the cyclic voltammetric response to the analyte. The shape of the voltammogram is due to the concentration of the reactant (R) or product (P) at the electrode surface during the scan. Ideally, the scan begins at a potential of negligible current flow whereby the analyte is neither oxidized nor reduced. As the potential is ramped linearly, electron transfer between the electrode and the analyte in the solution begins to occur; this leads to an accumulation of product and a depletion of the reactant. The ramp increases in accordance to the Nernst Equation.

$$E = E^0 + \frac{0.059}{n} \log \frac{[OX]}{[Red]}$$

Where E is the applied potential and E^0 the formal potential; [OX] and [Red] represent surface concentrations at the electrode solution interface, not bulk solution concentrations. Note that the Nernst equation may or may not be obeyed depending on the system or on the experimental conditions.

At the peak of the anodic wave the reaction becomes diffusion controlled, as the diffusion layer has grown sufficiently from the electrode that the flux of the product to the electrode is too slow to satisfy the Nernst equation. As a result, the concentration of the reactant at the surface reaches zero. Subsequently, the rate of diffusion then decreases, reducing the current flow, in accordance with the Cottrell equation. Once the potential ramp has reached the switching potential, the potential is ramped in the opposite direction resulting in a cathodic potential being applied.

The peak current for a reversible system is described by the Randles-Sevcik equation [66]. The current is directly proportional to the concentration and increases in respect to the square root of the scan rate. This dependence on scan rate implies the reaction at the electrode is controlled by mass transport. The equation applies at standard temperatures. (25°C, n = number of electrons involved, A = electrode area, D = diffusion coefficient, C_B = bulk electrode concentration and v = scan rate).

$$i_p = (2.69 \cdot 10^5) n^{\frac{3}{2}} A D^{\frac{3}{2}} C_B v^{\frac{1}{2}}$$

The reversibility of an electrochemically reversible couple can be identified by the measurement of the potential difference between the two peak potentials. An electrochemically reversible system based on a one electron transfer process is denoted in equation A. A fast one electron transfer exhibits a ΔE_p of 59 mV.

$$\Delta E_p = E_{pa} - E_{pc} = \frac{59}{n} \text{ mV}$$

1.10.2 Amperometry

A fixed potential is applied to an electrode against a reference electrode (Fig 1.17a.) until a steady state current is generated. This is achieved more readily in a stirred solution due to the greater efficiency of mass transport. Stirring also ensures that the concentration gradient at the working electrode is constant. Once steady state is achieved, standard additions of the analyte of interest are added into the voltammetric cell. The additions result in increases in current, with each addition occurring after steady state has been achieved, the magnitude of the current is proportional to the concentration of the analyte, which in turn is proportional to the rate of the redox reaction at the working electrode surface. An example of a typical amperometric plot is shown in Figure 1.17.b.

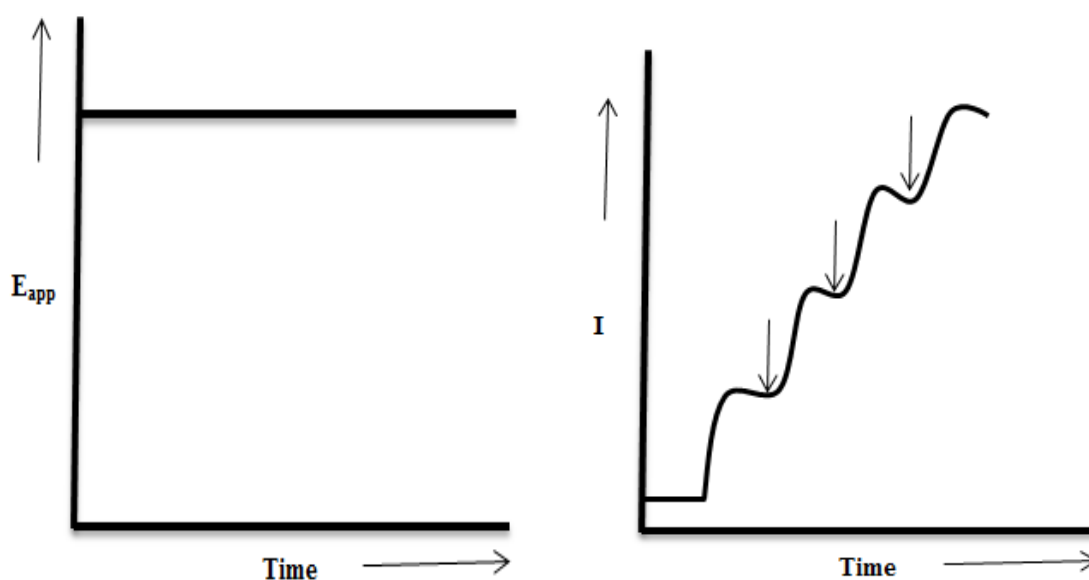


Figure 1.17: (a) Current waveform for amperometric experiments. (b) A typical amperometric plot in stirred solution. Arrows indicate additions of the target analyte.

1.10.3 Chronoamperometry

Chronoamperometry differs from amperometry by being conducted in a quiescent, unstirred solution. A sufficient E_{app} is applied to drive a redox reaction at the surface (Figure 1.18a); this generates a large current which decays rapidly as the concentration of the analyte is depleted at the electrode surface due to the diffusion (Fig 1.18b).

The variation in the magnitude of current with time for a planar electrode is described by the Cottrell equation [67], which is derived from Fick's second law. The equation is described as follows; n represents the number of electrons, F is the Faraday constant, A is the electrode area (cm^2), C° is the bulk electrolyte concentration (mol/cm^3), t is time (seconds) and D is the diffusion coefficient (cm^2/s).

$$i_t = \frac{nFAC^\circ D^{\frac{1}{2}}}{\pi^{\frac{1}{2}} t^{\frac{1}{2}}}$$

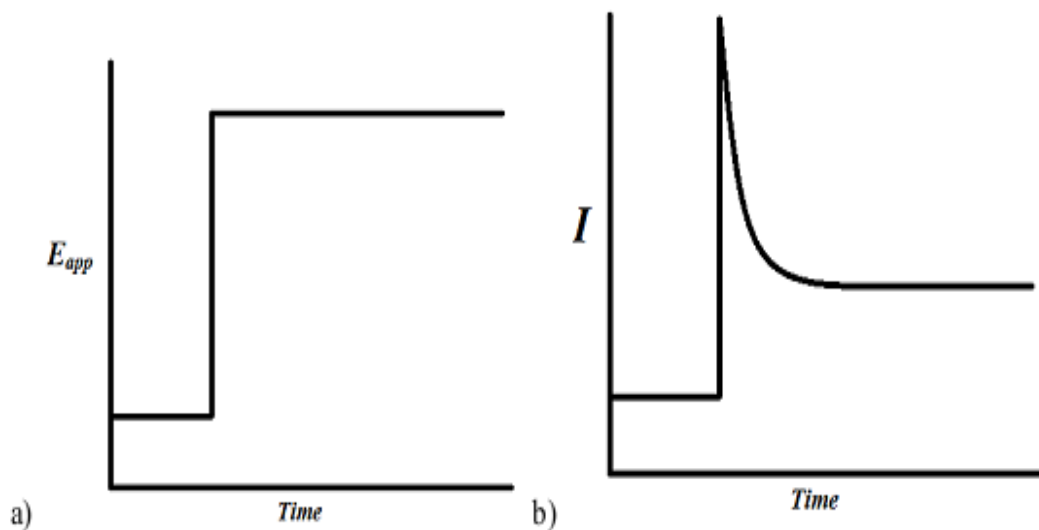


Fig 1.18: a) excitation wave from b) current response output generated from the excitation waveform.

1.11 Sensor characterization

1.11.1 Scanning electron microscopy (SEM)

The scanning electron microscope (SEM) is a powerful and frequently used instrument, in both academia and industry, to study, for example, surface topography, composition, crystallography and properties on a local scale. The spatial resolution is better than that of the optical microscope although not quite as good as for the transmission electron microscope (TEM). The SEM has an extremely large depth of focus and is therefore well

suites for topographic imaging. Besides surface topographic studies the SEM can also be used for determining the chemical composition of a material, its fluorescent properties, the formation of magnetic domains and so on. The specimen is bombarded by a convergent electron beam, which is scanned across the surface. This electron beam generates a number of different types of signals, which are emitted from the area of the specimen where the electron beam is impinging (Fig. 1.19).

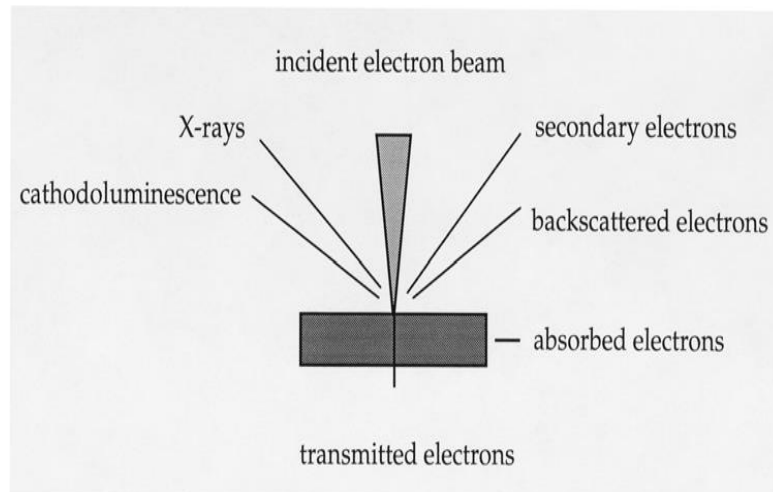


Figure 1.19: Different types of signals produced when high-energy electron impinges on a material.

The induced signals are detected and the intensity of one of the signals (at a time) is amplified and used to as the intensity of a pixel on the image on the computer screen. The electron beam then moves to next position on the sample and the detected intensity gives the intensity in the second pixel and so on.

The working principle of the SEM is shown in Figure 1.20. For improved signal-to-noise ratio in the image, one can use a slower scan speed. This means that the electron beam stays a longer time at one position on the sample surface before moving to the next. This gives a higher detected signal and increased signal-to-noise ratio.

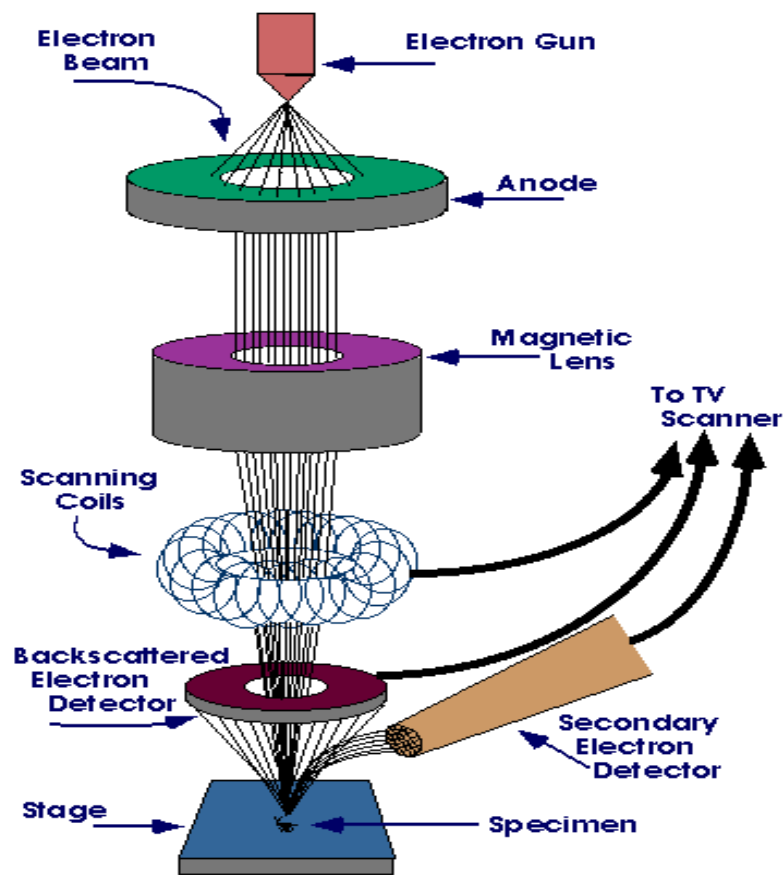


Figure 1.20: Schematic diagram of a SEM [67].

1.11.2 X-ray diffraction (XRD)

X-ray diffraction (XRD) relies on the dual wave/particle nature of X-rays to obtain information about the structure of crystalline materials. A primary use of the technique is the identification and characterization of compounds based on their diffraction pattern.

The dominant effect that occurs when an incident beam of monochromatic X-rays interacts with a target material is scattering of those X-rays from atoms within the target material. In materials with regular structure (i.e. crystalline), the scattered X-rays undergo constructive and destructive interference. This is the process of diffraction. The diffraction of X-rays by crystals is described by Bragg's Law, $n(\lambda) = 2d \sin(\theta)$. The directions of possible diffractions depend on the size and shape of the unit cell of the material. The intensities of the diffracted waves depend on the kind and arrangement of atoms in the crystal structure.

However, most materials are not single crystals, but are composed of many tiny crystallites in all possible orientations called a polycrystalline aggregate or powder. When a powder with randomly oriented crystallites is placed in an X-ray beam, the beam will see all possible interatomic planes. If the experimental angle is systematically changed, all possible diffraction peaks from the powder will be detected.

The parafocusing (or Bragg-Brentano) diffractometer is the most common geometry for diffraction instruments. This geometry offers the advantages of high resolution and high beam intensity analysis at the cost of very precise alignment requirements and carefully prepared samples. Additionally, this geometry requires that the source-to-sample distance be constant and equal to the sample-to-detector distance. Alignment errors often lead to difficulties in phase identification and improper quantification. A mis-positioned sample can lead to unacceptable specimen displacement errors. Sample flatness, roughness, and positioning constraints preclude in-line sample measurement. Additionally, traditional XRD systems are often based on bulky equipment with high power requirements as well as employing high powered X-ray sources to increase X-ray flux on the sample, therefore increasing the detected diffraction signals from the sample. These sources also have large excitation areas, which are often disadvantageous for the diffraction analysis of small samples or small sample features.

1.12 Objectives of the present work

The objective of this research is to develop a H_2O_2 sensor and also to study the sensitivity, selectivity, stability of this sensor using various electrochemical techniques.

The specific aims are:

- i) To synthesis of SnO_2 nanoparticles by hydrothermal method.
- ii) To synthesis of GO nanoparticles by modified Hummers method.
- iii) To modify Pencil graphite electrode with GO/ SnO_2 nanoparticle.
- iv) CV and amperometry has been used to study the analytical performance.
- v) To test and validate the modified sensor for the H_2O_2 .

CHAPTER II

Literature review

2.1. Introduction

Hydrogen peroxide is a very simple molecule, it is an important chemical and analyte in various industry fields, such as mining, environment, pharmaceutical, food manufacturing and textile applications. Meanwhile, H_2O_2 is also a kind of toxic by-product of many biological oxidases, based on which H_2O_2 has been considered to be an indicator of related diseases, such as Parkinson disease, cancer, stroke, arteriosclerosis and Alzheimer disease etc [68]. In addition, H_2O_2 has been applied in liquid-based fuel cells as an efficient oxidant and has also been employed in organic synthesis [69]. Therefore, it is one of the critical issues to detect H_2O_2 accurately for not only the academic research but also the industrial purpose. Electrochemical techniques conquer these shortcomings and provide more convenient detection processes according to the amperometric sensors. However, the slow kinetics and high overpotential on traditional solid electrodes could largely reduce the H_2O_2 sensing performance [70]. To improve the sensitivity, selectivity and stability of the sensing interface, chemically modified electrodes with highly active catalysts have been rapidly developed and widely applied to the electrochemical sensors.

The sensitivity of the assay can be tailored by altering the length of the accumulation step. Short accumulation times, in the order of less than one minute, can be used to determine sub to high ppm levels, with ppb and even sub ppb levels can be determined if the accumulation time is extended. The aim of this present study was to investigate the possibility of using pencil electrode for the anodic CV and amperometric determination of H_2O_2 . The voltammetric behavior of H_2O_2 at the electrode was first investigated by CV. The optimum conditions required for the CV and amperometric determination of H_2O_2 were then identified and finally the possibility of determining of H_2O_2 . This allows for an extremely facile, green, low-cost, rapid method to fabricate electrode prototypes, as illustrated.

A number of different carbon based materials and technologies have been commonly utilized such as glassy carbon [71], carbon paste [72], or screen-printed [73]. All of these approaches require some degree of expertise, preparation and care. As a result, a number of alternative sources for the manufacture of carbon electrodes have been investigated, such as the utilization of pencil leads as electrodes [74-76]. The pencil "lead" is actually a mixture of graphite, wax and clay, the proportions of which impart different properties to the pencil with increasing amounts of clay making the pencil harder, hence the designation 'H'. Increasing the levels of graphite make the pencil softer, and their marks darker or black and so the designation 'B'. For example, one of the darkest generally available pencils, the 6B is 84% graphite, 10% clay and 5% wax, compared to the common, lighter HB, or No. 2 pencil which has a composition of 68% graphite, 26% clay and 5% wax [77]. Commonly, pencils have been used directly as the working electrode itself, only recently has the possibility of using pencils to draw electrodes and other electronic components onto a suitable substrate been reported [78]. This latter approach has a number of advantages, as designs and geometries can be easily altered as they are simply drawn by hand on to a suitable substrate. This latter approach has a number of advantages, as designs and geometries can be easily altered as they are simply drawn by hand on to a suitable substrate.

A number of different electrochemical applications including resistors, capacitors, UV and piezoresistive sensors, microfluidic devices, chemiresistive sensors, biosensors, batteries and field effect transistors have been reported [93]. However, there have only been a small number of reports on the application of these devices using voltammetry and until now its application has been generally only in the characterization of the electrode [79].

In the recent years, there has been observed an increasing trend for the applications of GPE based electrodes in the environmental analysis. To the best of our knowledge, this is the first review article that covers environmental analytical applications of GPE.

Hence, this review gives brief description of

- Basic electrochemistry of Graphene and Enzymes.
- Graphene based electrode for small Biomolecules (hydrogen peroxide, NADH, dopamine, etc).

- Graphene based enzyme biosensors have been summarized in more detail; Graphene-based DNA sensing and environmental analysis have been discussed.
- Properties of the GPE and modified GPEs which enhance the sensitivity and selectivity of the electrode toward particular target species.

2.2. Basic electrochemistry of graphene

For the potential application of a certain kind of carbon material in electrochemistry, the basic electrochemical behaviors should be first studied to determine several important parameters of carbon electrodes [79, 80, 81]: electrochemical potential window, electron transfer rate, redox potentials, etc.

Based on Zhou report [82], graphene exhibits a wide electrochemical potential window of ca. 2.5 V in 0.1 M PBS (pH 7.0) [82], which is comparable to that of graphite, glassy carbon (GC), and even boron-doped diamond electrodes [79, 80, 82], and the charge-transfer resistance on graphene as determined from AC impedance spectra is much lower than that of graphite and GC electrodes [82].

The electron transfer behavior studies of graphene using cyclic voltammetry (CV) of redox couples, such as $[\text{Fe}(\text{CN})_6]^{3-/4-}$ and $[\text{Ru}(\text{NH}_3)_6]^{3+/2+}$, are reported, which exhibit well-defined redox peaks [87 – 89]. Both anodic and cathodic peak currents in the CVs are linear with the square root of the scan rate, which suggests that the redox processes on graphene-based electrodes are predominantly diffusion-controlled [88]. The peak-to-peak potential separations (ΔE_p) in CVs for most one-electron-transfer redox couples are quite low, very close to the ideal value of 59 mV, for example, 61.5 – 73 mV (10 mV/s) for $[\text{Fe}(\text{CN})_6]^{3-/4-}$ [87, 89, 90] and 60 – 65 mV (100 mV/s) for $[\text{Ru}(\text{NH}_3)_6]^{3+/2+}$ [89], much smaller than that on GC [79]. The peak-to-peak potential separation is related to the electron transfer (ET) coefficient [91], and a low ΔE_p value indicates a fast ET for a single-electron electrochemical reaction [90] on graphene. In order to study the electrochemical response/activity of graphene toward different kinds of redox systems, Tang [89] systematically studied three representative redox couples: $[\text{Ru}(\text{NH}_3)_6]^{3+/2+}$, $[\text{Fe}(\text{CN})_6]^{3-/4-}$, and $\text{Fe}^{3+}/\text{Fe}^{2+}$. As is known, $[\text{Ru}(\text{NH}_3)_6]^{3+/2+}$ is a nearly ideal outer-sphere redox system that is insensitive to most surface defects or impurities on electrodes and can serve as a useful benchmark in comparing electron transfer of various carbon electrodes; $[\text{Fe}(\text{CN})_6]^{3-/4-}$ is “surface-sensitive” but not “oxide-sensitive”; and $\text{Fe}^{3+}/\text{Fe}^{2+}$ is both “surface-sensitive”

and “oxide-sensitive” [79]. The apparent electron-transfer rate constants (k^0) calculated from CV on graphene and GC electrodes are 0.18 cm/s and 0.055 cm/s for $[\text{Ru}(\text{NH}_3)_6]^{3+/2+}$, respectively [89]. This indicates that the unique electronic structure of graphene, especially the high density of the electronic states over a wide energy range endows graphene with fast electron transfer [79]. The k^0 for $[\text{Fe}(\text{CN})_6]^{3-/4-}$, on graphene and GC were calculated to be 0.49 cm/s and 0.029 cm/s, respectively, and the electron transfer rates for $\text{Fe}^{3+/2+}$, at graphene electrode are several orders of magnitude higher than that at GC electrodes [89]. These indicate that the electronic structure and the surface physico-chemistry of graphene are beneficial for electron transfer [79, 89, 92].

2.3 Direct electrochemistry of enzymes

The direct electrochemistry of enzyme refers to the direct electron communication between the electrode and the active center of the enzyme without the participation of mediators or other reagents, which is very significant in the development of biosensors, biofuel cells and biomedical devices. However, the realization of direct electrochemistry of redox enzymes on common electrodes is very difficult because the active centers of most redox enzymes are located deeply in a hydrophobic cavity of the molecule. Carbon nanotubes and metal nanoparticles have exhibited excellent performance in enhancing the direct electron transfer between enzymes and electrodes, and are widely used [98]. Due to its extraordinary electron transport property (as shown in Section 2) and high specific surface area [94], functionalized graphene is expected to promote the electron transfer between electrode substrates and enzymes [95]. Shan [96] and Kang [97] reported the direct electrochemistry of glucose oxidase (GOD) on graphene.

Shan et al. [96] employed the chemically reduced graphene oxide (CR-GO) and Kang et al. [97] employed thermally split graphene oxide, both of which exhibit similar excellent direct electrochemistry of GOD. CVs of graphene, graphite-GOD, and graphene-GOD modified GC electrodes in PBS solution [95]. A pair of well-defined redox peaks was only observed at the graphene-GOD modified electrode, which is characteristic of reversible electron transfer process of redox active center (flavin adenine dinucleotide, FAD) in GOD, indicating that a direct electron transfer of GOD on graphene electrode has been successfully achieved. The formal potential ($E^{\circ'}$) calculated by averaging the cathodic and anodic peak potentials was estimated to be ca. -0.43 V (all the electrode potentials are vs.

Ag/AgCl, except specially stated), close to the standard electrode potential of FAD/FADH₂ [97]. The redox peaks of GOD have ca.69 mV peak-to-peak separation and ca. 1 ratio of cathodic to anodic current intensity [95], and peak current densities are in the linear relationship with scan rates [95, 97]. These indicate that the redox process of GOD on graphene electrode is a reversible and surface-confined process [97]. The electron-transfer-rate constant (k_s) of the GOD on graphene electrode is 2.83-0.18 s⁻¹, much higher than most of the values reported on carbon nanotubes [93], indicating that functionalized graphene provides fast electron transfer between the redox center of the enzyme and the surface of electrode [97]. Graphene electrodes exhibit a high enzyme loading (1.12-10⁻⁹ mol/cm²) due to its high surface area [97]. This is advantageous for increasing the sensitivity of graphene-based biosensors. The direct electron transfer of GOD on graphene is stable, for example, no obvious changes in 15 cycles on the cyclic voltammetric responses of the GOD– graphene – chitosan modified electrode in N₂-saturated PBS (pH 7.4) and the response retention of above 95% after 1 week storage [97]. The excellent performance of graphene toward the direct electrochemistry of GOD indicates that graphene is a potential promising material for enzyme electrodes.

2.4. Graphene-based electrodes for small biomolecules

2.4.1. Hydrogen Peroxide (H₂O₂)

H₂O₂ is a general enzymatic product of oxidases and a substrate of peroxidases, which is important in biological processes and biosensor development [99]. Hydrogen peroxide is also an essential mediator in food, pharmaceutical, clinical, industrial, and environmental analyses [99]; therefore, it is of great importance to detect

H₂O₂. The key point in developing electrodes for detecting H₂O₂ is to decrease the oxidation/reduction overpotentials. Kinds of carbon materials, such as carbon nanotubes [93], have been developed in constructing biosensors for detecting H₂O₂. Graphene has shown promise in this aspect.

Zhou et al. [99] studied the electrochemical behavior of hydrogen peroxide on graphene (chemically reduced graphene oxides, CR-GO) modified electrode, which shows a remarkable increase in electron transfer rate compared with graphite/GC and bare GC electrodes [99]. As shown in CVs in Figure 3, the onset potentials of

H₂O₂ oxidation/reduction on CR-GO/GC (a1), graphite/GC (b1), and GC electrodes (c1) are 0.20/0.10 V, 0.8 V, and 0.70 V, respectively, indicating superior electrocatalytic activity of graphene toward H₂O₂.

The linear relationship of H₂O₂ at -0.2 V on CR-GO/GC electrode is 0.05 – 1500 mM, wider than the previously reported results for carbon nanotubes [99]. These can be attributed to the high density of edge-plane-like defective sites on graphene, which might provide many active sites for electron transfer to biological species [93]. Such significantly enhanced performance on graphene-based electrodes for detecting H₂O₂ may lead to high-selectivity/- sensitivity electrochemical sensors.

Gi Hun Seong developed electrochemical microfluidic devices containing Au-Ag bimetallic nanoparticles on single-walled carbon nanotube (SWCNT) electrodes for precise, rapid and non-enzymatic electrochemical detection of hydrogen peroxide (H₂O₂). A homogeneous SWCNT layer on a glass substrate was patterned by a standard photolithography method and an O₂-plasma technique. The patterned SWCNT layers were used as working electrode, counter electrode, and reference electrode in a 1 mm wide and 23 μm deep microchannel. To enhance the electrochemical catalytic properties of the working electrode, Au covered Ag nanoparticles (NPs) were electrochemically deposited on the SWCNT working electrode with current streaming solution into a microfluidic channel. The AgNPs had catalytic activity to improve the reduction of H₂O₂ combined with AuNPs, which could support catalytic reaction of AgNPs. The reduction in H₂O₂ in fabricated devices was monitored at an optimized condition and was linear with H₂O₂ concentration, resulting in a sensitivity of 13.1 μA·cm⁻²·mM⁻¹, a correlation coefficient of $r^2 = 0.985$, and limit of detection 26.8 μM (S/N = 3). For the analysis of real samples, diluted antiseptic solutions containing 3 wt% H₂O₂ were used to determine the concentration of H₂O₂ in the pharmaceutical sample. The recovery values ranged from 97% to 107%, and relative standard deviations were below 5%. The developed microfluidic sensor is a prospective electrochemical platform for accurate, reproducible non-enzymatic detection of H₂O₂.

Yimin Sun et al. recently developed a facile and effective method to fabricate a new type of flexible and lightweight electrode based on the sputter deposition of ultrafine Pt nanoparticles on free-standing rGO-CNT paper. Owing to the synergistic effect of

different components in the Pt/rGO–CNT paper, the resultant nano-hybrid paper exhibited excellent mechanical, physicochemical and electrochemical properties. When used as a freestanding paper electrode for flexible electrochemical biosensor, the Pt/rGO–CNT electrode demonstrated a remarkably improved sensing performance in comparison with Pt/rGO paper and commercial Pt foil electrode toward H_2O_2 , and can be used for real-time tracking H_2O_2 secretion by live cells macrophages. Furthermore, it is worth to mention that our strategy for the preparation of free-standing Pt/rGO–CNT paper is expected to be a modular approach to fabricate the graphene-based paper with multi-functional components, which has a great potential for the development of high performance implantable biochemical devices, flexible energy conversion units, on-chip power sources, flexible lithium ion batteries, supercapacitor, and other electronic systems.

Manan et al. recently developed a new Ni^{2+} based metal organic framework (AP-Ni-MOF) material was successfully synthesized and characterized by different analytical techniques, including IR spectroscopy, EDS, XRD, SEM and TGA. The synthesized MOF material was modified to a carbon paste electrode and employed as an electrochemical sensor for sensing H_2O_2 . Under an optimum condition, the voltammetric reduction of H_2O_2 at AP-Ni-MOF/CPE in phosphate buffer solution has been studied. Under selected conditions, there was a linear relationship between the peak current and certain concentration range (0.004 to 60mM) of H_2O_2 with low LOD (0.0009 mM). Moreover, it also showed good reproducibility, stability and good selectivity. In addition, high percentage recovery (94.7 to 107%) in real samples (lens cleaner solutions), suggested that the AP-Ni-MOF modified to CPE is a promising method to improve the CPE material in electrochemical analysis and extend its application in the scope electrochemical sensing.

Siva et al. reported a demonstrated the possibility to develop an electrochemical sensor based on CS-AgNWs to detect H_2O_2 and a respective enzyme biosensor for glucose adding glucose oxidase enzyme. The resultant modified electrodes exhibited good catalytic performance toward H_2O_2 reduction. The enzyme electrodes are easily fabricated by immobilizing GOx onto the CS-AgNWs which exhibits excellent enzyme accommodation; it also allows the direct electron transfer between the redox centers of the enzyme with the modified electrode surface. Moreover, chitosan plays a crucial role in stabilizing and immobilizing GOx. The electrocatalytic activity of modified electrode with high sensitivity can be successfully exploited for monitoring glucose levels in blood.

Takeshi Kondo et al. reported a conductive boron-doped diamond (BDD) thinfilm has been expected as an alternative electrode material for electro-analysis, due to its attractive properties; wide potential window, low background current, as well as physical stability and chemical inertness. Thus, high sensitive analytical results have been reported for many types of electro-active species, from metals to bio-related organic compounds. In order to expand the applicability for electro-analysis of BDD electrodes, immobilizing functional materials, such as catalytic metals, metal oxides and enzymes, on the surface have been investigated. As is generally known, as-prepared CVD diamond surfaces are hydrogen-terminated, and the surfaces can be oxidized with various oxidation treatments to form oxygen-containing surface functionalities. The functionalities on diamond surfaces are considered to exhibit some reactivity comparable to those of organic compounds, thus they can be used for generating covalent bonds to immobilize functional molecules. In this study, ferrocene, which has been known as a good electron mediator, was covalently immobilized on BDD electrode surfaces, and the properties for a hydrogen peroxide sensor were investigated. BDD thin films were prepared on n-type highly conductive silicon wafer substrates by means of microwave plasma-assisted (MP) CVD method. The carbon source was a mixed solution of acetone and methanol (9:1, v/v), with dissolved B_2O_3 (10,000 ppm B/C atomic ratio). Oxidation of BDD surfaces were carried out by employing a laboratory-made UV-ozone cleaner, which consists of a chamber to fill oxygen gas with a low-pressure Hg lamp. Immobilization of ferrocene derivatives were achieved with esterification between ferrocenecarboxylic acid and hydroxyl group on UV-ozone treated (50 min.) BDD surfaces with dicyclohexylcarbodiimide (DCC) method. For electrochemical measurement, a conventional electrochemical glass cell with a Pt wire and an Ag/AgCl electrode as a counter and reference electrodes, respectively, was used. Voltammetry was carried out using a digital potentiostat.

Mohammad fabricated an electrochemical sensor for H_2O_2 determination was prepared by electrodepositing copper oxide nanoparticles on the activated pencil graphite electrodes. At first, a study has been made of the optimum conditions for chemical activation of the pencil graphite electrodes (APGE) and then the activated pencil graphite electrode was modified with copper oxide nanoparticles (CuO/APGE) and used as a non-enzymatic hydrogen peroxide sensor. The morphology of the modified electrode surface was investigated by scanning electron microscopy (SEM). Upon the addition of H_2O_2 , the

modified electrode (CuO/APGE) exhibits significant oxidation of H₂O₂ with starting potential around +0.05 V (vs. Ag/AgCl) which dramatically decreases the overpotential of H₂O₂ oxidation. Under the optimal experiment conditions, the electrocatalytic response current of this sensor was proportional to the H₂O₂ concentration in the range of 5.0×10^{-6} to 1.6×10^{-3} mol L⁻¹ with a detection limit down to 0.21 μmol L⁻¹ (signal/noise = 3). The sensitivity was calculated to be 4.75 μAL mmol⁻¹. The electrochemical active surface area and the catalytic rate constant of hydrogen peroxide electro-oxidation were calculated. The H₂O₂ sensor exhibited a low detection limit, a good signal reproducibility (relative standard deviation (RSD), n = 4) 2.36 % and the accurate measurements in milk as the real sample.

2.4.2. NADH

B-nicotinamide adenine dinucleotide (NAD) and its reduced form (NADH) are a cofactor of many dehydrogenases [100], which has received considerable interest in developing amperometric biosensors, biofuel cells, and bioelectronic devices associated with NAD/NADH-dependent dehydrogenases. The oxidation of the NADH serves as the anodic signal and regenerates the NAD cofactor, which is of great significance in bio sensing important substrates such as lactate, alcohol or glucose [101].

Problems inherent to such anodic detection are the large overvoltage for NADH oxidation and surface fouling associated with the accumulation of reaction products [101]. Graphene shows promise in addressing these problems. Tang [102] studied the electrochemical behavior of NADH on graphene (chemically reduced graphene oxides, CR-GO) modified electrode, which shows a remarkable increase in electron transfer rate compared with graphite/ GC and GC electrodes [102]. The peak potentials of NADH oxidation is shifted from 0.70 V on GC and graphite to 0.40 V on CR-GO [102]. These are attributed to the high density of edge-plane-like defective sites on CRGO, which provide many active sites for electron transfer to biological species.

Liu reported a further enhanced performance of graphene-based electrode toward the oxidation of NADH through increasing the dispersity of graphene via noncovalent functionalization of graphene with methylene green (MG).

The oxidation of NADH on MG-graphene electrode takes place ~ 0.14 V, which is much lower than that (~ 0.40 V) for pristine graphene (i.e., without MG functionalization) and carbon nanotubes based biosensors [93].

The enhanced activity of graphene modified electrodes toward NADH oxidation is further confirmed in Lin et al. report when compared with bare edge plane pyrolytic graphite electrode (EPPGE) which has many edge-plane-like defective sites [103]. It is known that the high density of edge-plane-like defective sites, which might provide many active sites for electron transfer to biological species, contribute to the enhanced activity of carbon materials toward oxidation/reduction of small biomolecules such as NADH [104]. The higher activity of functionalized graphene modified EPPGE than bare EPPGE indicates that, in addition to the high density of edge-plane-like defective sites on graphene (chemically reduced graphene oxides), there are other special properties of graphene that contribute to its high activity. The exact mechanisms still need more investigation. Pumera report [105] on high-resolution X-ray photoelectron spectroscopy (HRXPS) and ab initio molecular dynamics study of adsorption of NAD⁺/NADH (Figure 5) might provide preliminary insight into this. It shows that the adsorption of NAD⁺ molecules on the edges of graphene is attributed to the interaction with oxygen-containing groups such as carboxylic groups, while graphene edges substituted only with hydrogen are prone to passivation [105]. Therefore, the oxygen-containing groups might play one key role for the enhanced activity of graphene.

2.4.3 Dopamine

Dopamine (DA), an important neurotransmitter, plays a significant role in the central nervous, renal, hormonal, and cardiovascular systems [93]. Its detection has gained significant attention. Rapid, simple, and sensitive electrochemical methods have shown promising in the neurotransmission detection. However, at traditional solid electrodes,

DA and its coexisting species ascorbic acid (AA) and uric acid (UA) have an overlapping voltammetric response, resulting in rather poor selectivity and sensitivity of DA. Plane sites/defects that occur at the end of the vertical graphene nanoflakes, and their ability to act essentially as nanoconnectors that electrically transport the electrons to the underneath substrate [106].

Alwarappan [107] reported that graphene exhibited a better sensing performance toward dopamine than SWCNTs and can effectively distinguish AA, DA, and ST (serotonin). This is attributed to the presence of more sp²-like planes and various edge defects present on the surface of graphene [107].

Wang reported that graphene exhibited high selectivity for sensing dopamine with a linear range of 5 nM– 200 nM, and a better performance than multiwalled carbon nanotubes. They attributed it to the high conductivity, high surface area and π – π stacking interaction between dopamine and graphene surface [108].

2.5. Graphene-based electrochemical sensors

The excellent electrochemical behaviors of graphene indicate graphene is a promising electrode material in electroanalysis [79]. Several electrochemical sensors based on graphene and graphene composites for bioanalysis and environmental analysis have been developed [95, 82, 97].

2.5.1. Graphene-based enzyme biosensors

On the basis of the high electrocatalytic activity of graphene toward H₂O₂ and the excellent performance for direct electrochemistry of GOD, graphene could be an excellent electrode material for oxidase biosensors. Several graphene-based glucose biosensors have been reported [93].

Shan [95] reported the first graphene-based glucose biosensor with graphene/polyethylenimine-functionalized ionic liquid nanocomposites modified electrode which exhibits wide linear glucose response (2 to 14 mM, R² 0.994), good reproducibility (relative standard deviation of the current response to 6 mM glucose at -0.5 V was 3.2% for 10 successive measurements), and high stability (response current ±4.9% after 1 week) [95].

Zhou [82] reported a glucose biosensor based on chemically reduced graphene oxide (CR-GO). Graphene (CR-GO)-based biosensor exhibits substantially enhanced amperometric signals for sensing glucose: wide linear range (0.01 – 10 mM), high sensitivity (20.21 mA/mMcm²) and low detection limit of 2.00 mM (S/N=43). The linear range for glucose detection is wider than that on other carbon materials-based electrodes, such as carbon nanotubes [109] and carbon nanofibers [110]. The detection limit for glucose at the

GOD/CR-GO/GC electrode (2.00 mM at -0.20 V) is lower than that of some reported carbon materials-based biosensors, such as carbon nanotubes paste, carbon nanotubes nanoelectrode, carbon nanofiber [110], exfoliated graphite nanoplatelets, and highly ordered mesoporous carbon [111]. The response at the GOD/CR-GO/GC electrode to glucose is very fast (9 s to steady-state response) and highly stable (91% signal retention for 5 h), which makes GOD/CR-GO/GC electrode a potential fast and highly stable biosensor to continuously measure the plasma glucose level for the diagnosis of diabetes.

Kang et al. [97] employed biocompatible chitosan to disperse graphene and construct glucose biosensors. It was found that chitosan helped to form a well-dispersed graphene suspension and immobilize the enzyme molecules, and the graphene-based enzyme sensor exhibited excellent sensitivity ($37.93 \text{ mA} \cdot \text{M}^{-1} \cdot \text{cm}^{-2}$) and long-term stability for measuring glucose.

Graphene/metal nanoparticles (NP) based biosensors have also been developed. Shan et al. [112] reports a graphene/AuNPs/chitosan composites film based biosensor which exhibited good electrocatalytic activity toward H_2O_2 and O_2 . Wu et al. [113] reports GOD/graphene/PtNPs/chitosan based glucose biosensor with a detection limit of 0.6 mM glucose. These enhanced performance were attributed to the large surface area and good electrical conductivity of graphene, and the synergistic effect of graphene and metal nanoparticles [113].

The excellent catalytic activity of functionalized graphene toward NADH oxidation indicates that graphene is a promising material for dehydrogenase biosensors. Zhou et al. [99] reports an ethanol biosensor based on graphene-ADH. The ADH-graphene-GC electrode exhibits faster response, wider linear range, and lower detection limit for ethanol detection compared with ADH-graphite/GC and ADH/GC electrodes. This enhanced performance can be explained by the effective transfer of substrate and products through graphene matrixes containing enzymes as well as the inherent biocompatibility of graphene [99].

2.5.2. Graphene-based electrochemical DNA biosensors

Electrochemical DNA sensors offer high sensitivity, high selectivity and low cost for the detection of selected DNA sequences or mutated genes associated with human disease, and promise to provide a simple, accurate and inexpensive platform of patient diagnosis. Electrochemical DNA sensors also allow device miniaturization for samples with a very small volume [113]. Among all kinds of electrochemical DNA sensors, the one based on the direct oxidation of DNA is the simplest [91, 92].

Zhou [92] reported an electrochemical DNA sensor based on graphene (chemically reduced graphene oxide). As shown in, the current signals of the four free bases of DNA (i.e., guanine (G), adenine (A), thymine (T), and cytosine (C)) on the CR-GO/GC electrode are all separated efficiently, indicating that CR-GO/GC can simultaneously detect four free bases, but neither graphite nor glassy carbon can. This is attributed to the antifouling properties and the high electron transfer kinetics for bases oxidation on CR-GO/GC electrode [92] which results from high density of edge-plane-like defective sites and oxygen-containing functional groups on CR-GO that provide many active sites and are beneficial for accelerating electron transfer between the electrode and species in solution [93]. This is attributed to the unique physicochemical properties of CR-GO (the single sheet nature, high conductivity, large surface area, antifouling properties, high electron transfer kinetics, etc.) [92].

2.5.3. Graphene-based electrochemical sensors for heavy metal ions

Graphene-based electrochemical sensors have been developed for environmental analysis for the detection of heavy metal ions (Pb^{2+} and Cd^{2+}) [115]. Li [114, 115] report that Nafion-graphene composite film based electrochemical sensors not only exhibit improved sensitivity for the metal ion (Pb^{2+} and Cd^{2+}) detections, but also alleviate the interferences due to the synergistic effect of graphene nanosheets and Nafion [115].

The stripping current signal is greatly enhanced on graphene electrodes. As shown in the differential pulse anodic stripping voltammograms (DPASV) in, the stripping current signal is well distinguished. The linear range for the detection of Pb^{2+} and Cd^{2+} is wide. The detection limits ($S/N = 3$) are 0.02 mg L^{-1} for both Pb^{2+} and Cd^{2+} , which are more sensitive than those of Nafion film modified bismuth electrode [115], and ordered mesoporous

carbon coated GCE[118], and comparable to Nafion/CNT coated bismuth film electrode [118]. The enhanced performance is attributed to the unique properties of the graphene (nanosized graphene sheet, nano-scale thickness of these sheets and high conductivity), which endowed the capability to strongly adsorb target ions, enhanced the surface concentration, improved the sensitivity, and alleviate the fouling effect of surfactants [114, 115].

Table 2.1: Some recent applications of PGE electrodes

Electrode composition	Linear range (μM)	Detection limit (μM)	Sensitivity $\mu\text{Acm}^{-2}\text{mM}^{-1}$	Working Potential V	Year	Ref
N-graphene	0.5–1200	0.05		-0.4	2011	[120]
CuS/rGO	5–1500	0.27	26.5	-0.27	2013	[121]
rGO – Pt	0.5–3475	0.2	459	-0.08	2014	[122]
Fe ₃ O ₄ /rGO	1–20,000	0.17	387.6	-0.3	2014	[123]
Co ₃ O ₄ –rGO	15–675	2.4	1140	-0.19	2014	[124]
GO/Au@Pt@Au	0.05–17,500	0.02		+0.5	2015	[125]
rGO-PMS@AuNPs	0.5–50,000	0.06	39.2	-0.75	2014	[126]
Pt/rGO–CNT paper	0.1–25	0.01	1.41	-0.25	2015	[127]
rGO–Au–PTBO	5–1077.1	0.2	63.39	-0.3	2013	[128]
3D graphene/pDA/TH	0.4–660	0.08	169.7	- 0.25	2013	[129]
SnO ₂ -GO/PGE	1-7	0.09	0.534	-0.4	This paper	

2.6. Attractive features and challenges of graphite pencil electrodes

GPE possesses many attractive and unique features which make it an excellent choice for electrochemical sensing. These features are summarized below.

- A unique feature is the provision of the renewable surface after each measurement just like the dropping mercury electrode. This feature makes the electrode surface foul free. But in the case of most of other electrodes like GCE, after each electrochemical measurement, a number of by-products are formed which can adhere to the surface of the electrode and could compromise the

sensitivity of the electrode. However, here in case of GPE, the part of the used electrode can be easily removed, and the new surface is readily available.

- The surface polishing is generally not required prior to use. [130]
- The GPE is easily available [131] as it is widely used for writing purposes as a graphite pencil.
- It is also disposable [131] like screen-printed electrode. However, it is extremely low cost [132] compared to disposable SPE.
- Handling of GPE is relatively easy, and due to its elongated shape, the direct electro-modification methods are more facile. [133]
- GPE is found more sensitive compared to GCE [132] (greater sensitivity is due to the presence of porosity on the surface of GPE).
- The control of the sensing area is also possible by changing the extruded pencil length.

Despite its excellent behavior and the advantages, the GPE is facing few problems. Still, it is not a well-established electrode, and it is not prepared for electrode applications, due to this reason, sometimes the electrode composition may vary. This could affect the sensor behavior. Such issues can be fixed by preparing the graphite pencil typically for electrode purposes. The modification by casting method is also challenging due to the smaller diameter of a pencil. Although there are some challenges associated with GPE, the GPE can be an excellent commercial electrode due to the above attractive features for the study of environmental pollutants. It has the capability to overcome the regeneration problem of the other solid state electrodes. [130]

2.7. Future scope and outlook

Point of care (POC) testing has become the most well-known way of diagnosis in clinical analysis, food safety, and the environment. The main advantage of POC lies in the fact that it provides results in very short time compared to centralized laboratories. These devices are helpful in making quick decisions. The water that is considered to be a matrix of life has been highly polluted with inorganic and organic impurities in different parts of the globe due to the industrial revolution. This fact has already been indicated by a number of published reports [134]. Similarly, thousands of publications talk about analytical method

development for analysis of enzyme and non-enzyme sensor in water, food [135] and biological samples [136]. Hence, there is very high stress on existing analytical technologies to meet the demands of low cost, availability, sensitivity and applicability in on field analysis. GPE based electrochemical devices can have the potential to serve in POC applications. Their low cost, easy availability, and trait of disposability make them quite fit for POC based devices. Despite low cost and commercial availability of GP based electrodes, the commercialization of readily available GPE sensors for real life samples is still at some distance from the reality. Every lab prepared prototype cannot be brought to the market without considering its suitability for the desired assay, study of consumables and acceptability by the consumers. Although electrochemical methods involving modified GPEs demonstrate a grade of maturity good enough to implement them in real analytical applications but up till now, their applications are limited to proof of concepts. For a proof of concept, different materials such as nanoparticles, conductive polymers, and carbon-based materials have been used to modify the surface of GPEs. However, which of them can be employed for mass production of modified GPEs for certain analysis will be dictated by cost, ease of synthesis and stability of the material over the electrode surface. Moreover, the integration of such modified electrodes into miniaturized systems is nothing less than a challenge as commercialization needs careful designing of the product that should be compatible with market demands. Thus, these challenges need to be addressed in future.

CHAPTER III

Experimental Section

3.1. Materials

All chemicals and solvents are used in the synthetic and analytical works were of analytical grade obtained from E. Merck, Germany, Qualikems Fine chem Pvt. Ltd, Loba chem pvt. Ltd, and Sigma-Aldrich, India. The used chemicals were- Sodium thiosulfate, Disodium hydrogen phosphate (Na_2HPO_4), Sodium dihydrogen phosphate ($\text{NaH}_2\text{PO}_4 \cdot 2\text{H}_2\text{O}$) were purchased from Sigma-Aldrich, India. Di-phosphorus pentoxide (P_2O_5), Potassium permanganate (KMnO_4), Phosphoric acid (H_3PO_4), Potassium peroxydisulfate ($\text{K}_2\text{O}_8\text{S}_2$), Hydrochloric acid (HCl), Sulfuric acid (H_2SO_4), Ammonia solution was obtained from MERCK, Germany. Graphite powder was obtained from Qualikems Fine Chem. Pvt. Ltd. India. Stannous chloride dehydrate ($\text{SnCl}_2 \cdot 2\text{H}_2\text{O}$) was obtained from Loba chem. India. For cleaning and all other purposes distilled water was used. All chemicals were used as supplied except purification of the solvent.

3.2. Equipments

CV and amperometry measurements were performed with a potentiostat/Galvano stat (model: μstat 8400, Drop sens), Spain. There are three electrode cells has been used, Where Tin-oxide and Graphene oxide modified pencil graphite electrode ($\text{SnO}_2\text{-GO/PGE}$) was employed as a working electrode with Ag/AgCl and Pt were as reference and counter electrodes, respectively.

3.3. Preparation and polishing of pencil graphite electrodes (PGEs)

Various grade (2B, 3B, 4B, HB) pencil graphite was used in this study. Fill the electrode were tested in 1mM Ferricyanide solution to understand the electrochemistry of PGEs.

A cutter was used to make the pencil graphite electrode from the pencil graphite. The lead was then rinsed with distilled water to remove any trace of adhesive. The exposed surface served as the point of attachment of the PGEs to the potentiostat.

Finally, the wood from the top about 1.5 cm of the pencil was carefully removed using a small razor blade, until the pencil lead was fully exposed. The lead was then rinsed successively with acetone and distilled water to remove any traces of adhesive. This exposed surface served as the point of attachment of the PGEs to the potentiostat. The exposed PGE tip polished on 150-grit sandpaper for 10 minutes and rinsed with ethanol and distilled water.

3.4. Synthesis of SnO₂ nano crystal

For the hydrothermal synthesis of SnO₂ nanoparticles, dissolving of 2g (0.1M) stannous chloride dehydrate (SnCl₂.2H₂O) in 100 mL distilled water. After complete solution, ammonia solution was added to the above solution by drop wise under stirring. The resulting gels were filtered and dried at 80°C for 24 hours. In order to remove water molecules. Finally, tin oxide nano-powders were formed at 550°C for 2h. [36].

3.5. Preparation of GO

Graphene oxide was prepared by a modified two-step Hummers method [37] using natural graphite powder. Graphene oxide was prepared from the pre-oxidized graphite. Typically, 5.0 g graphite powder was dissolved in 7.5 mL concentrated H₂SO₄ at 80 °C under vigorous stirring. 2.5 g K₂S₂O₈ and 2.5 g P₂O₅ was then added into the black solution. After reaction for 3 h, the mixture was cooled down to room temperature and then diluted, filtered and washed. The product was dried in vacuum at 60°C Over 24 h.

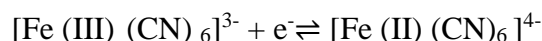
In an ice bath, 3 g KMnO₄ was slowly added in the solution of pre-oxidized graphite (1.0 g) and 23 mL concentrated H₂SO₄ under vigorous stirring. Then 27.6 mL deionized water was injected into the product and the mixture became olive after stirring at 35 °C for 2h. The solution was further diluted by adding 84 ml deionized water, followed by the addition of 1.5 mL H₂O₂ (30%). Finally, the solution was filtered with 150 ml HCl (1:10) after it was cooled to room temperature. The yellow product was dried and dissolved in deionized water. After dialyzed for 4 days, the brown product was dried for further use. Finally, reduced graphene oxide powder were formed at 350 °C for 10 minutes.

3.6. Modification of working electrode

PGE is used in this study for electrode modification using rGO-SnO₂. The modified electrode was prepared by a simple casting method [38]. Prior to the surface coating, the PGE was polished on 150 –grit sand paper a substantial amount of graphite was removed, respectively, and was rinsed with water, followed by sonication in ethanol solution and water successively. A mixture of rGO-SnO₂, chitosan and Nafion was dropped on to the clean surface of PGC, and was dried at room temperature for overnight.

3.7. Standardization of the electrochemical System

The whole electrochemical set-up was tested using a standard experiment. In the standard experiment we have studied the following redox couple at a PGE electrode.



The reaction above was studied electrochemically by pumping electrons into the system from a PGE electrode and by measuring the change in the flow of current during the reaction. This is done most conveniently by scanning the potential of the electrode at a constant rate.

In general, the peak current of diffusion controlled reversible or quasi-reversible electro - chemical reaction follows Randles–Sevcik equation;

$$I_p = 0.4463nF \sqrt{\frac{nFD}{RT}} AC\sqrt{v}$$

Where i_p : the peak current, n : the number of electrons, F : Faraday constant, T : the temperature in Kelvin, R : the gas constant, A : the surface area of the working electrode, D : the diffusion coefficient of the electro active species, C : the bulk concentration of the electro active species and v : the scan rate of voltammograms.

CHAPTER IV

Results and Discussion

4.1. Electrochemical setup standardization

Cyclic voltammograms (CVs) of ferricyanide at 3B pencil graphite electrode (PGE) (Figure 4.1) were performed at concentration of 2mM of ferricyanide 0.1 M KNO_3 as supporting electrolyte, each solution was scanned at different scan rate equal to 20, 40, 60, 80, 100, 120, 140, 160 mV/s.

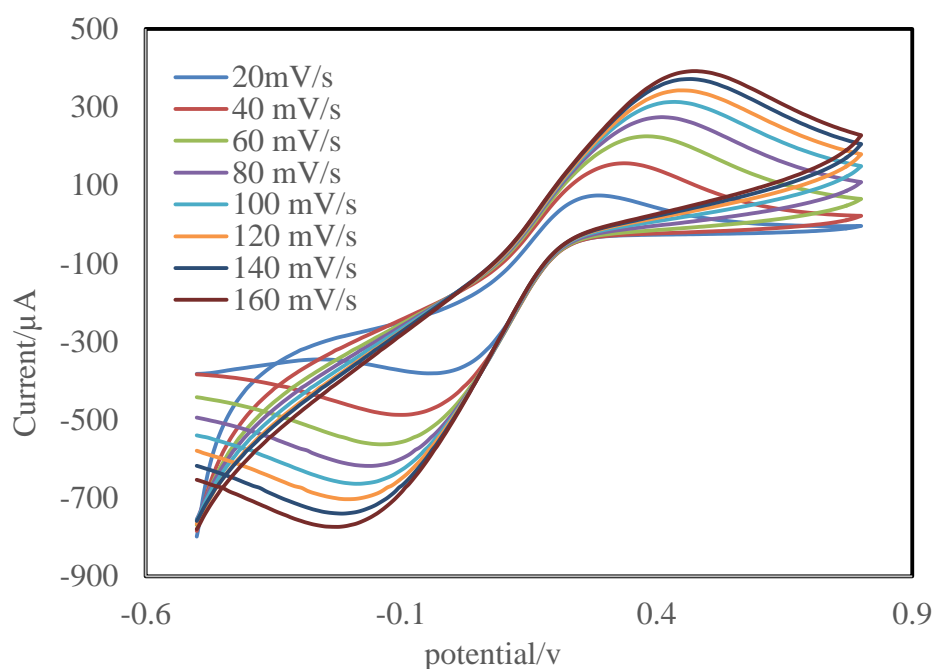


Fig.4.1(a): CV of ferricyanide at 3B pencil graphite electrode were performed at concentration of 2mM of ferricyanide 0.1 M KNO_3 as supporting electrolyte, different scan rate 20, 40, 60, 80, 100, 120, 140, 160mV/s.

When the scan rate increases, current is also increases. We show that the experimental value of surface area is very close to theoretical value. The physical properties of pencil graphite electrodes that are described the look or feel of a substance. Electrode was made

from locally available and cheap pencil graphite instead of conventional costly platinum, gold or glassy carbon electrodes.

Chemical properties that are relate to the ability of a substance to react with other substances or to transform from one substance to another. The chemical properties of a substance relate to its chemical composition and the way the atoms in the molecules are chemically bonded together. A pencil can write on certain objects, namely paper the eraser will melt the metal near the eraser will conduct heat pencil lead is usually Amorphous graphite and graphite's chemical properties include conduct electricity [137].

$$\text{Surface area of pencil graphite} = \pi r^2$$

Although π is approximately 3.14, in this activity we will use $\pi = 3.14$ for calculations.

Table 4.1: Electrochemical parameters obtained from voltammograms of Fig. 4.1(a)

ν Vs^{-1}	$\nu^{1/2}$	E_{pa} V (+)	E_{pc} V (+)	i_{pa} μA (+)	i_{pc} μA (-)	i_{pa}/i_{pc}
0.02	0.141421	0.28	0.10	100.706	-100.279	1.00
0.04	0.200000	0.28	0.10	127.080	-120.791	1.05
0.06	0.244949	0.27	0.11	196.451	-179.375	1.09
0.08	0.282843	0.29	0.11	218.451	-200.250	1.09
0.1	0.316228	0.27	0.11	246.958	-210.541	1.17
0.12	0.34641	0.29	0.13	254.416	-215.291	1.18
0.14	0.374166	0.31	0.13	260.492	-255.333	1.02
0.16	0.400000	0.31	0.12	264.582	-256.000	1.03

ν = scan rate; $\nu^{1/2}$ = SQRT of scan rate; E_{pa} = anodic peak potential; E_{pc} = cathodic peak potential ; i_{pa} = anodic peak current; i_{pc} = cathodic peak current.

In general, the peak current of diffusion controlled reversible or quasi-reversible electro-chemical reaction follows Randles–Sevcik equation

$$I_p = 0.4463nF \sqrt{\frac{nFD}{RT}} AC\sqrt{v} \quad \dots\dots\dots (1)$$

Where i_p : the peak current, n : the number of electrons, F : Faraday constant, T : the temperature in Kelvin, R : the gas constant, A : the surface area of the working electrode, D : the diffusion coefficient of the electroactive species, C : the bulk concentration of the electroactive species and v : the scan rate of voltammograms.

Thus, if we know the value of diffusion coefficient of ferricyanide at 298K the surface areas for ferricyanide are calculated from the slope of the plot of I_p versus \sqrt{v} (Fig. 4.1).

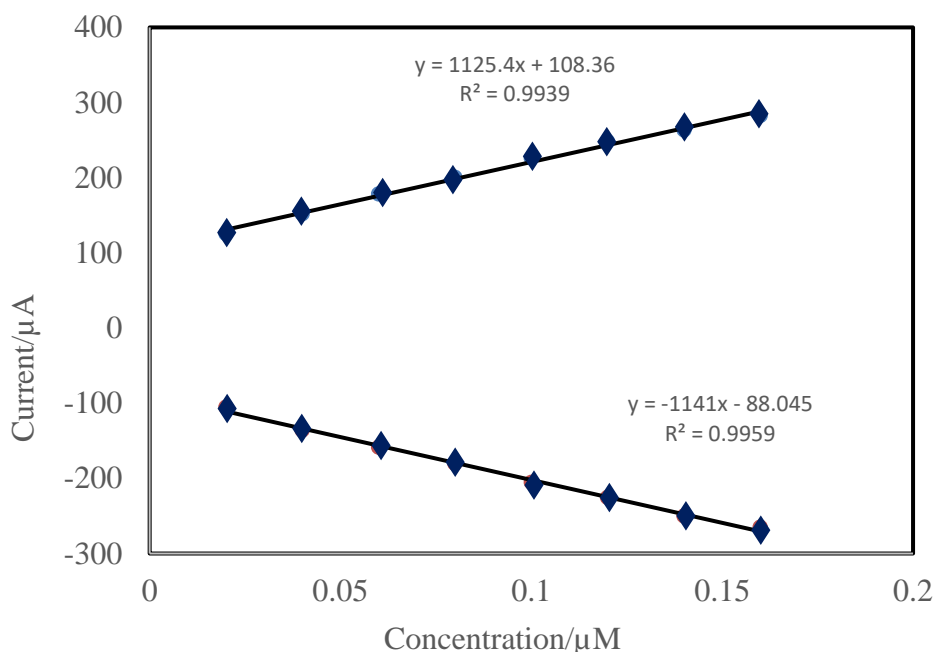


Fig.4.1 (b): The anodic and the cathodic peak heights as function of the square root of the scanning rate for pencil graphite electrode.

From Equation (1) we get,

$$\text{Slope} = 0.4463nF \sqrt{\frac{nFD}{RT}} AC$$

$$A = \frac{\text{Slope}}{0.4463nF \sqrt{\frac{nFD}{RT}} C}$$

From the curve (Fig 4.1) the value of slope is $\sim 545.6 \times 10^{-6}$ and the standard value of diffusion coefficient for ferricyanide in PGEs is $6 \times 10^{-9} \text{ cm}^2/\text{s}$. where concentration $C = 2 \times 10^{-4} \text{ mol}/\text{cm}^3$ so we get,

$$A = \frac{545.6 \times 10^{-6}}{0.4463 \times 1 \times 96500 \sqrt{\frac{1 \times 96500 \times 6 \times 10^{-9}}{8.314 \times 298}} \times 2 \times 10^{-4}}$$

$$A = 0.004 \text{ cm}^2$$

From the theoretical value the surface area of PGEs electrode i.e. used for experiment is 0.004 cm^2 . We show that the experimental value of surface area is very close to theoretical value. This calculated result has been used in further studies.

4.2. Synthesis of nanoparticle and its physical characterization

In the present study, rGO was synthesis by two step modified Hummers method and SnO_2 nanoclusters were synthesized through a hydrothermal process, in which graphene oxide was reduced to rGO and SnO_2 nanoclusters were in situ produced and deposited on the surface of rGO. The morphologies of the prepared materials were first characterized by SEM measurements. The SEM images of bare pencil graphite electrode and SnO_2 -rGO/PGE are shown in Figure 1. Compared to bare pencil graphite electrode (Figure 4.2 A), Figure 4.2 B depicts the SnO_2 -rGO mixer are deposit by drop casting on pencil lead surface. The average size of SnO_2 -rGO particles on pencil lead was 19.4 (5.5, $n=20$) nm. From comparison with bare pencil lead surface images, it was confirmed that most of pencil lead surface was covered with SnO_2 -rGO particles. The densely deposited SnO_2 -rGO nanostructures on pencil lead are expected to enhance the electrochemical activity. We also compared CV of the SnO_2 -rGO/PGE for $\text{Fe}(\text{CN})_6^{3-}$ (don't show the figure). Two CVs were almost identical indicating the deposited SnO_2 -rGO with a quite thin layer on pencil lead.

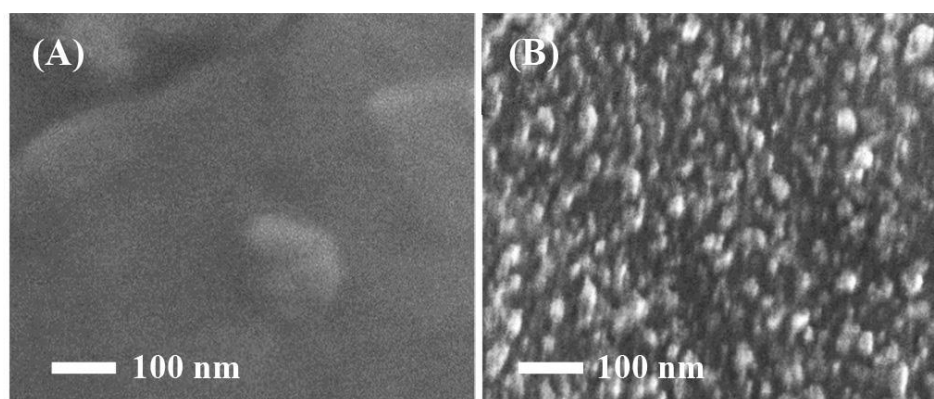


Fig.4.2: SEM micrographs of the surfaces of (A) bare pencil graphite electrode and (B) SnO_2 -rGO/PGE [138].

4.3. Sensor fabrication

A simple casting method has been used for the fabrication of GO-SnO₂/PGE [139]. At first, PGE was polished on 150-grit sandpaper until a substantial amount of graphite was removed and followed by washing with water and sonication in ethanol and water respectively. A mixture of 0.2 g GO and 0.2 g SnO₂ nanoparticle, 0.1g chitosan and 0.1 mL Nafion was dropped on to the clean surface of PGE, and dried at room temperature for overnight (Figure 4.3).

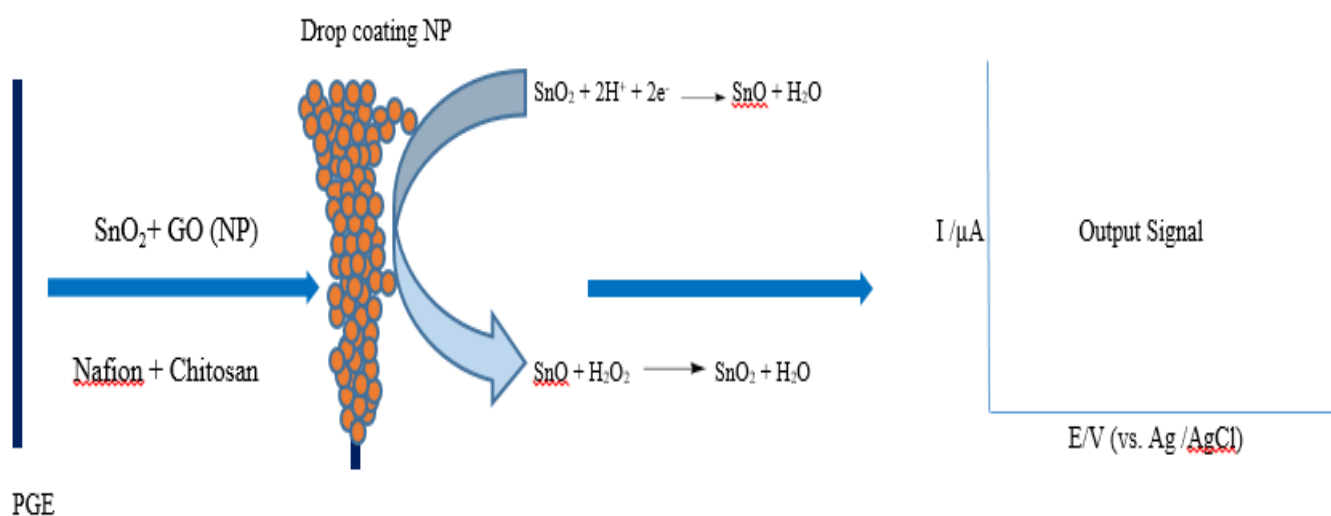


Figure.4.3: Schematic diagram of stepwise fabrication of the H₂O₂ sensor

4.4. Electrocatalytic activity of blank HB, 2B, 3B and 4B PGEs

The analytical applicability of the PGEs electrodes, we investigated the electrocatalytic activity of these electrodes towards H₂O₂. Fig. 4.4 presents the CV responses of blank HB PGEs in 0.1 M PBS without (a) and with H₂O₂ 0.1mM (b). In the absence of H₂O₂, no peak was observed. Upon the addition of H₂O₂, not an increase of the cathodic peak current density can be observed for PGEs electrode.

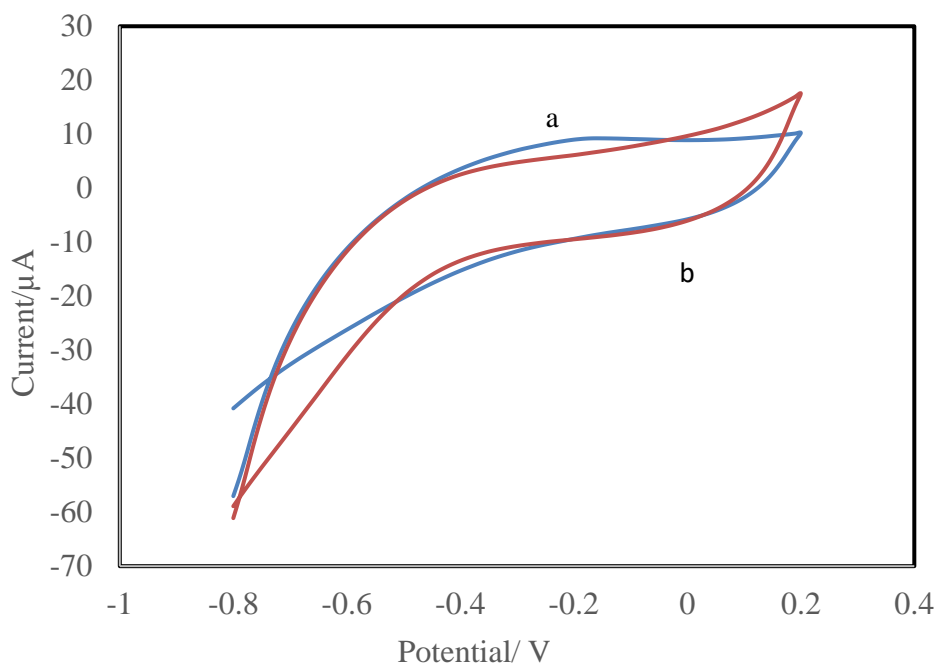


Fig. 4.4: CV curves in HB PGEs (a) in the absence of H₂O₂ and (b) in the presence of 0.1mM H₂O₂ in 0.1M phosphate buffer solution (pH=7.4) containing at $E_{app} = -1.0V$ (scan rate: 0.05 V/s).

It also can be seen that with the addition of H₂O₂, the cathodic peak not shifts to the higher potential, which may be attributing to the diffusion limitation of H₂O₂ at the electrode surface.

Fig. 4.5 presents the CV responses of blank 2B PGEs in 0.1 M PBS without (a) and with H₂O₂ 0.1mM (b). In the absence of H₂O₂, no peak was observed. Upon the addition of H₂O₂, not an increase of the cathodic peak current density can be observed for PGEs electrode.

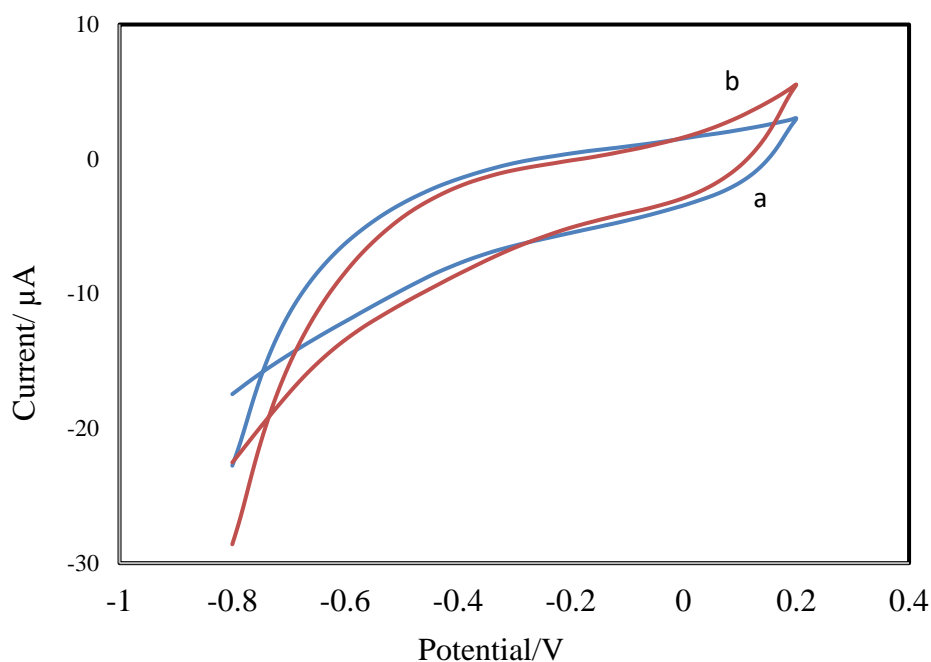


Fig. 4.5: CV curves in 2B PGC electrodes (a) in the absence of H_2O_2 and (b) in the presence of 0.1mM H_2O_2 in 0.1M phosphate buffer solution ($\text{pH}=7.4$) containing at $E_{\text{app}}=-1.0\text{V}$ (scan rate: 0.05 V/s).

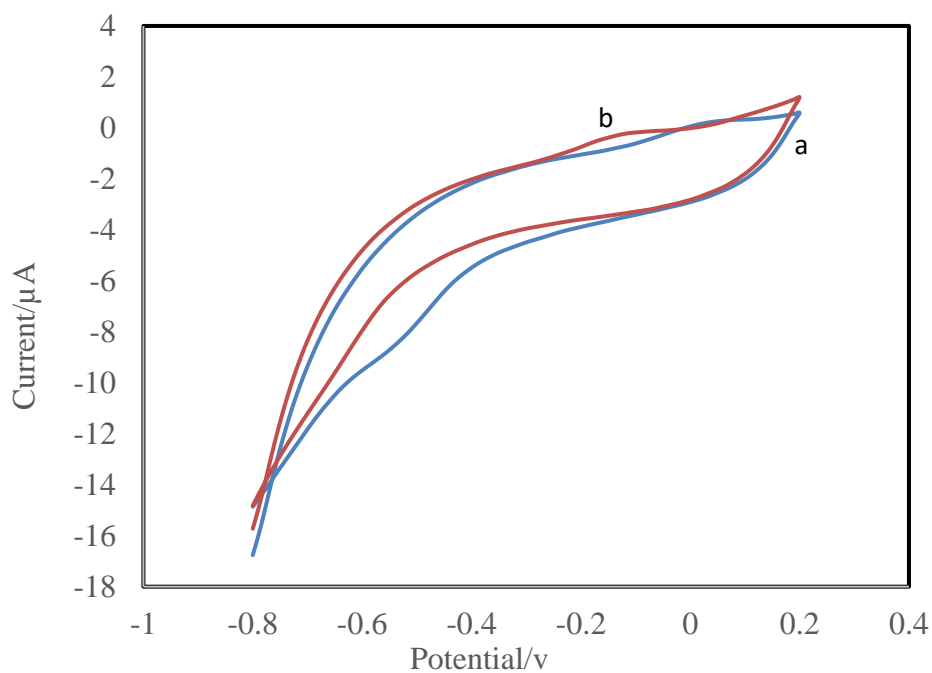


Fig. 4.6: CV curves in 3B PGC electrodes (a) in the absence of H_2O_2 and (b) in the presence of 0.1mM H_2O_2 in 0.1M phosphate buffer solution ($\text{pH}=7.4$) containing at $E_{\text{app}}=-1.0\text{V}$ (scan rate: 0.05 V/s).

Fig. 4.6 presents the CV responses of blank 3B PGEs in 0.1 M PBS without (a) and with H_2O_2 0.1mM (b). In the absence of H_2O_2 , no peak was observed. Upon the addition of H_2O_2 , not an increase of the cathodic peak current density can be observed for PGEs electrode

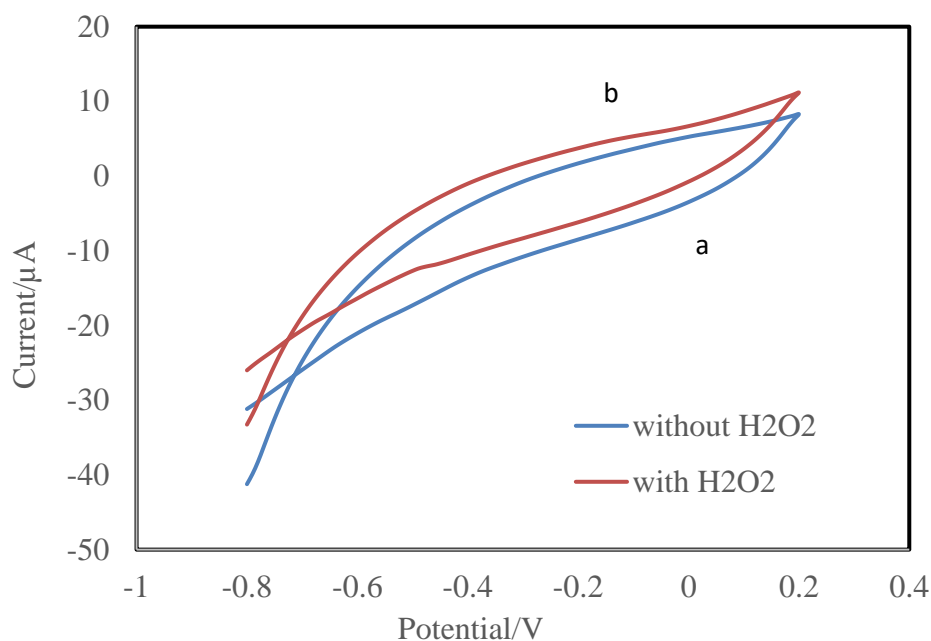


Fig. 4.7: CV curves in 4B PGC electrodes (a) in the absence of H_2O_2 and (b) in the presence of 0.1mM H_2O_2 in 0.1M phosphate buffer solution (Ph = 7.4) containing at $E_{\text{app}} = -1.0\text{V}$ (scan rate: 0.05 V/s).

Fig. 4.7 presents the CV responses of blank 4B PGEs in 0.1 M PBS without (a) and with H_2O_2 0.1mM (b). In the absence of H_2O_2 , no peak was observed. Upon the addition of H_2O_2 , not an increase of the cathodic peak current density can be observed for PGEs electrode

4.5 Catalytic Activity for H_2O_2 Reduction

As well known, the response time, detection sensitivity and selectivity, detection linear range, the limit of detection, practicability and reversibility etc. are the vital parameters for an electrochemical sensor.[140] Based on these, the sensing properties of $\text{SnO}_2\text{-rGO/PGE}$ for H_2O_2 detection were studied below.

To study the electrochemical properties of the SnO₂-rGO mixer and the application in electrochemical sensors, electrochemistry of graphite pencil electrode modified with the SnO₂-rGO was first examined in 0.1 M neutral (pH = 7.4) phosphate buffer solution (PBS) which is usually used in biomedical research and is close to the human body's pH. Fig. 4.8 shows the CVs of blank 3B PGE and SnO₂-rGO-modified PGE electrode (SnO₂-rGO/PGE) in 0.1 M PBS solution without and with 0.1 mM H₂O₂. It can be seen that on PGE electrode, no apparent current change can be observed when 0.1 mM H₂O₂ was added into the electrolyte, indicating the negligible catalytic activity of 3B PGE for H₂O₂ reduction. However, for SnO₂-rGO/PGE, there appears an obvious reduction current peak at around the addition of 0.1 mM H₂O₂ in the electrolyte. The cathodic current is obviously associated with the reduction of H₂O₂, suggesting the high catalytic activity of SnO₂-rGO for the electro-reduction of H₂O₂.

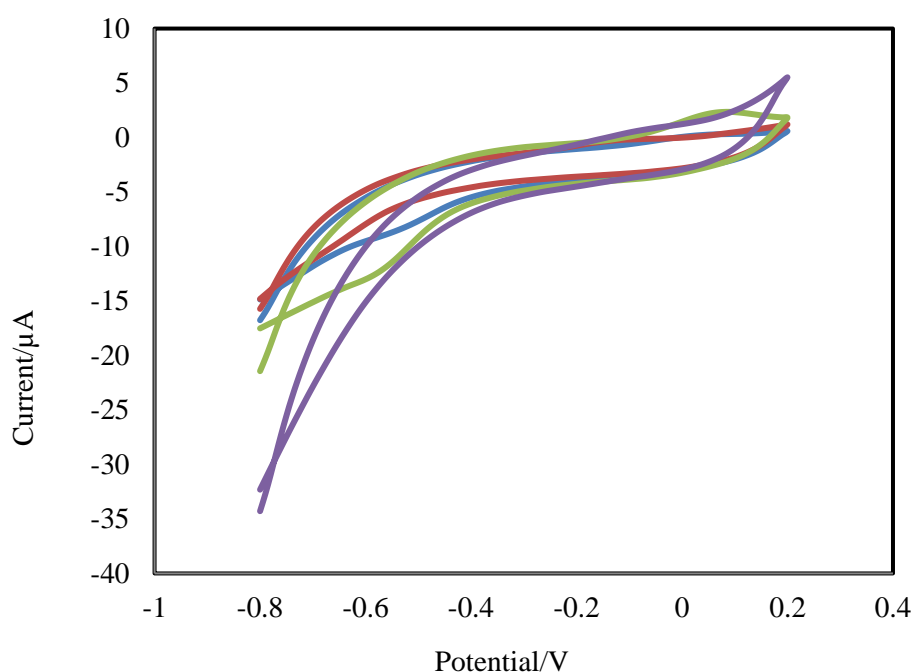


Fig.4.8: CV of blank 3B PGE and SnO₂-rGO/3B PGE in 0.1 M PBS (pH = 7.4) solution without and with 0.1 mM H₂O₂, potential scan rate 0.05 V s⁻¹.

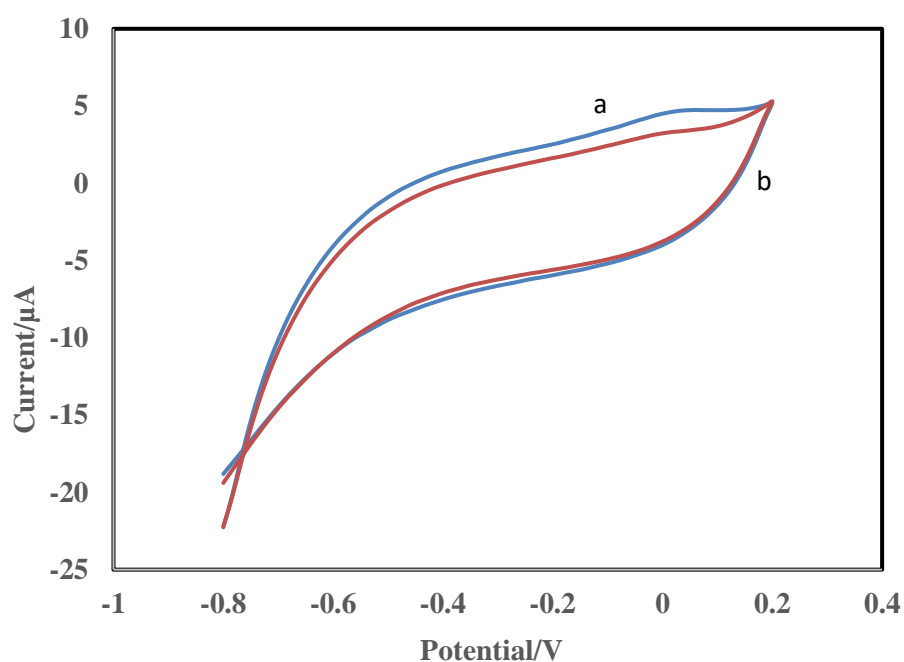


Fig.4.9: CV of rGO/3B PGE in 0.1 M PBS (pH = 7.4) solution without and with 0.1 mM H₂O₂, potential scan rate 0.05 V s⁻¹.

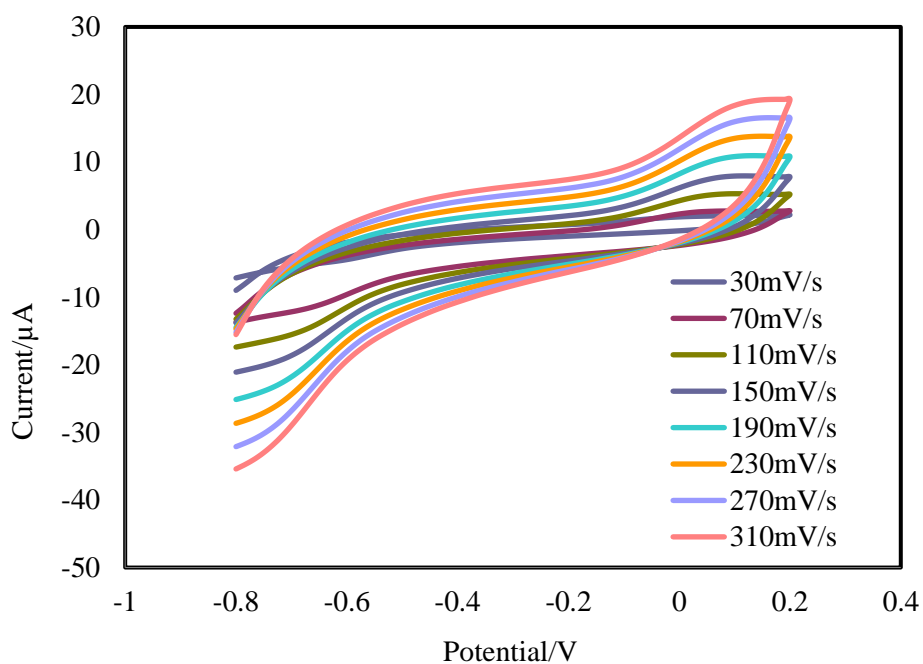


Fig.4.10: CV of different scan rates (30 to 310 mV/s) of SnO₂-rGO/3B PGE in 0.1 M PBS (pH = 7.4) solution without and with 0.1 mM H₂O₂, potential scan rate 0.05 Vs⁻¹.

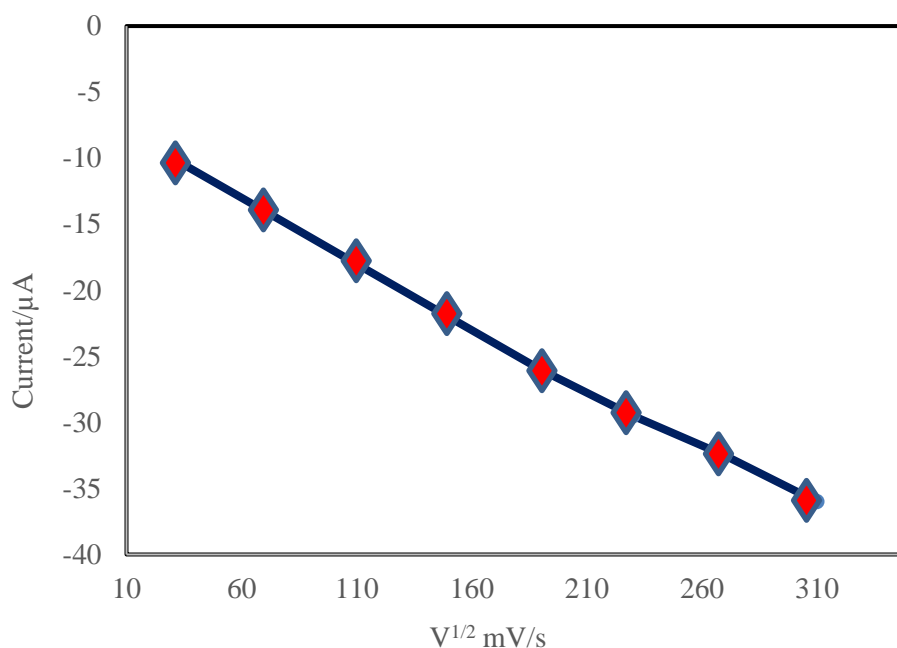


Fig.4.11: Dependence of H₂O₂ Reduced current on the square root of scan rate on SnO₂-rGO

With a control experiment, it can be seen from Fig. 4.9 that only a little increase of cathodic current appeared for rGO/PGE in 0.1 M PBS containing 0.1 mM H₂O₂. These results indicate that rGO has only low catalytic activity for H₂O₂ reduction. By using the electrocatalytic property of SnO₂-rGO, the high performance detection of H₂O₂ was achieved on the sensing platform fabricated from SnO₂-rGO. Moreover, in the present sensing material, the well-dispersion of small SnO₂ nanoclusters on rGO, the high conductivity of rGO, and the synergistic effect between SnO₂ and rGO are beneficial for enhancing the electrochemical activity for H₂O₂ reduction.

To explore the reaction kinetics of H₂O₂ reduction on the SnO₂-rGO hybrid material, CVs of rGO-SnO₂ 0.1 M PBS solution with 0.1 mM H₂O₂ at different scan rates were recorded in Fig. 4.10. It can be seen the reduction current increases gradually with the scan rate increased from 30 to 310 mV s⁻¹. As shown in Fig. 4.11, the peak current shows a linear relationship to the square root of potential scan rate, which suggests the reduction reaction of H₂O₂ is a diffusion-controlled process.

Fig. 4.12(a) displays the CVs for the electro-reduction of different concentrations of hydrogen peroxide at SnO₂-rGO/PGE electrode in 0.1 M PBS (pH=7.4) solution.

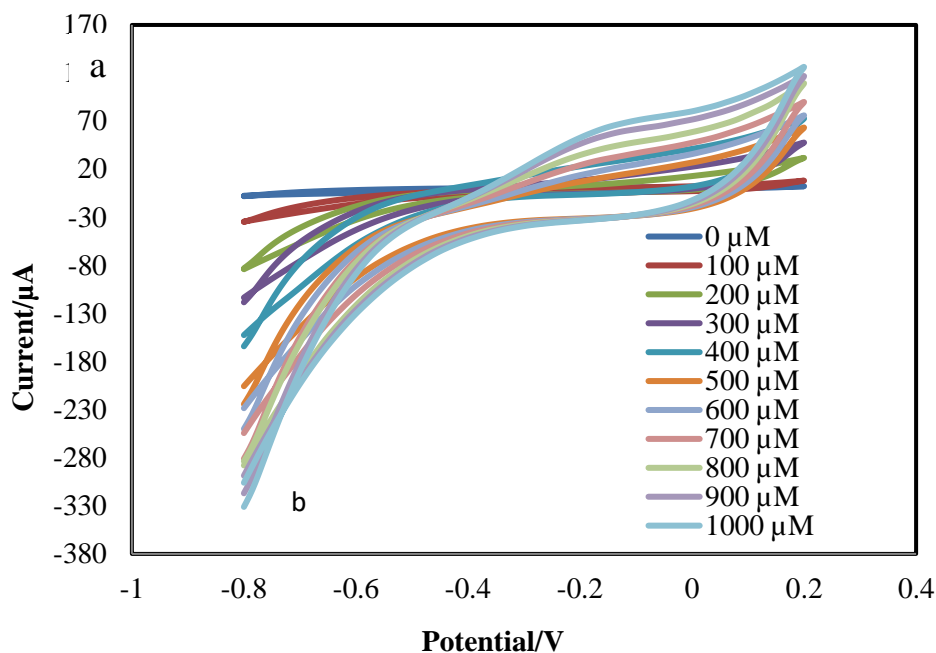


Fig. 4.12: (a) CV of SnO₂-rGO/PGE in 0.1 M PBS buffer solution containing different concentrations of H₂O₂ (from 0 to 1000 μM), potential scan rate 0.05 V s⁻¹.

It can be seen that the material is electrochemically sensitive to the concentration of hydrogen peroxide. Without the presence of H₂O₂ in electrolyte, only a featureless CV profile was obtained. With addition of 100 μM H₂O₂ into the PBS buffer solution, an obvious reduction current can be seen and the reduction current increases with the concentration of H₂O₂ increasing.

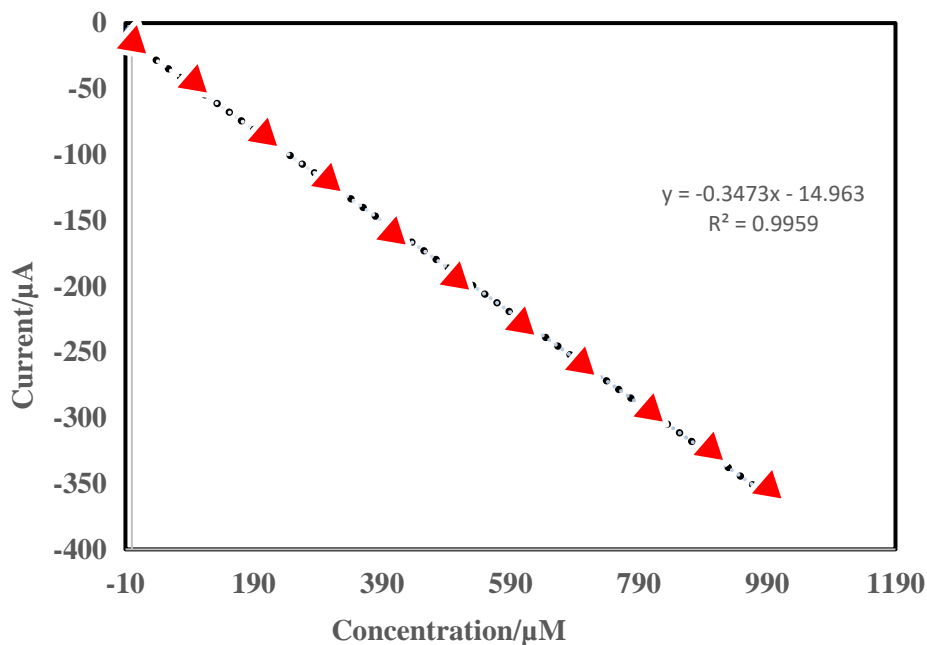
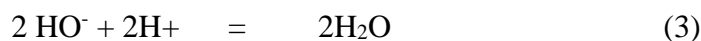


Fig. 4.12 : (b) Dependence of reduction peak current on the concentration of H₂O₂.

Fig. 4.12(b) shows the relationship between reduction peak current and the concentrations of added H₂O₂. A good linearity was obtained and the linear regression equation can be expressed as $Y = 0.3473x - 14.963$ ($R^2 = 0.9959$).

On the present SnO₂-rGO/PGE electrode, H₂O₂ could be reduced in the PBS solution through the following mechanism: [141]



Meanwhile, SnO₂-rGO may facilitate the electron transfer through the catalytic mechanism shown below:



In order to obtain a better understanding of the sensitivity of the H₂O₂ sensor the current response change with H₂O₂ concentrations was investigated. To further evaluate the sensing performance of the SnO₂-rGO mixer for hydrogen peroxide amperometric

detection, the current responses at a fixed potential (-0.4 V) to the addition of different concentrations of H_2O_2 in the electrolyte were recorded. Fig. 4.13 shows a typical amperometric response of the blank 3B PGE and 4.14 shows a typical amperometric response of rGO/PGE upon the successive addition of a certain concentration of H_2O_2 into stirred 0.1 M PBS (pH =7.4) solution. At the applied potential of -0.4 V, the blank 3B PGE and rGO/PGE gave no signal.

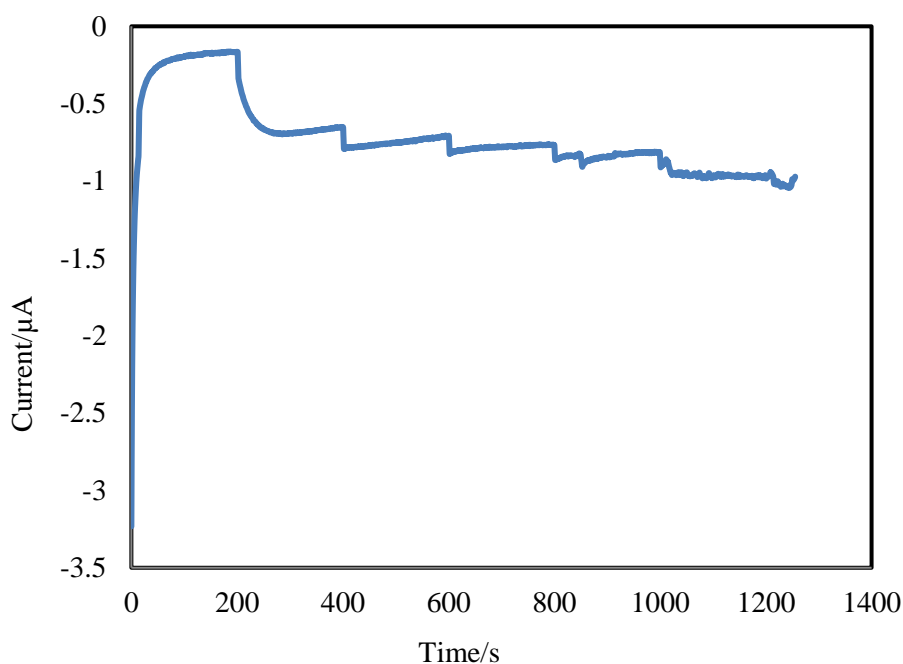


Fig. 4.13 : amperometric current response of the blank 3B PGEs upon the successive injection of H_2O_2 with concentrations from 1mM to 7 mM into a stirred at $E_{app} = -0.4\text{V}$ 0.1 M PBS pH 7.4.

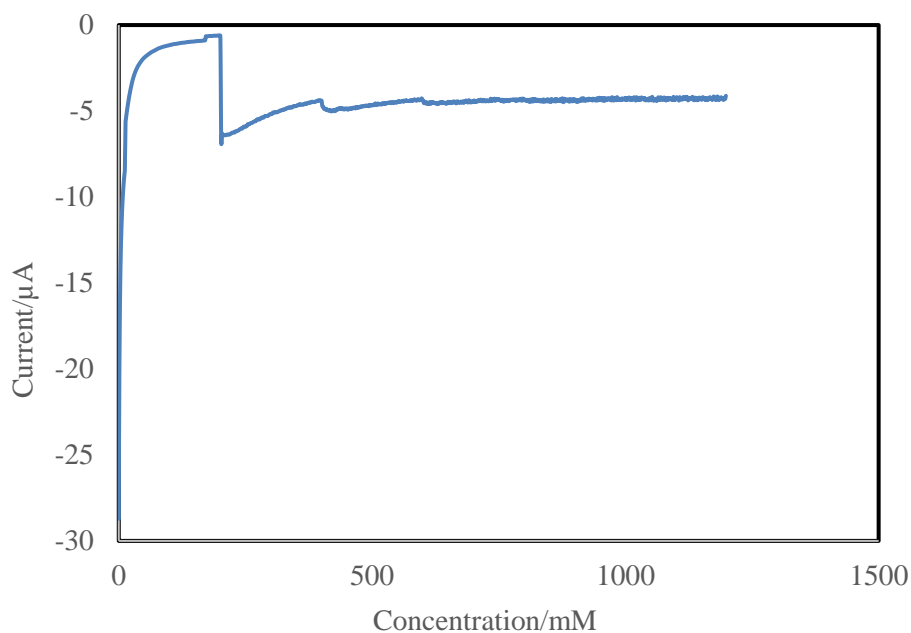


Fig. 4.14 : amperometric current response of rGO modified 3B PGE upon the successive injection of H₂O₂ with concentrations from 1mM to 7 mM into a stirred at $E_{app} = -0.4V$ 0.1 M PBS pH 7.4

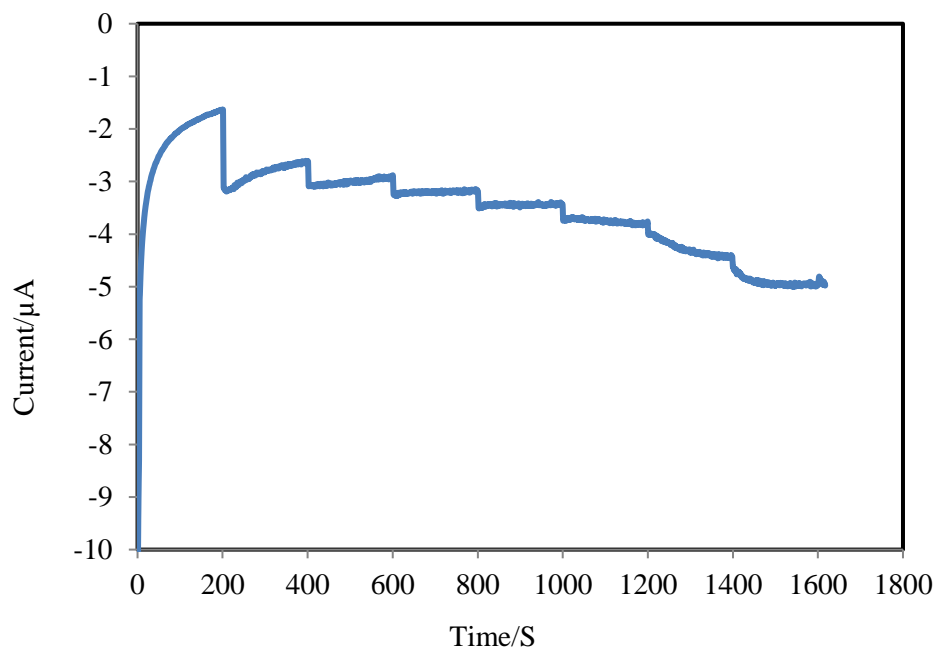


Fig. 4.15 : (a) amperometric current response of SnO₂ modified 3B PGE upon the successive injection of H₂O₂ with concentrations from 1mM to 7 mM into a stirred at $E_{app} = -0.4V$ 0.1 M PBS pH 7.4.

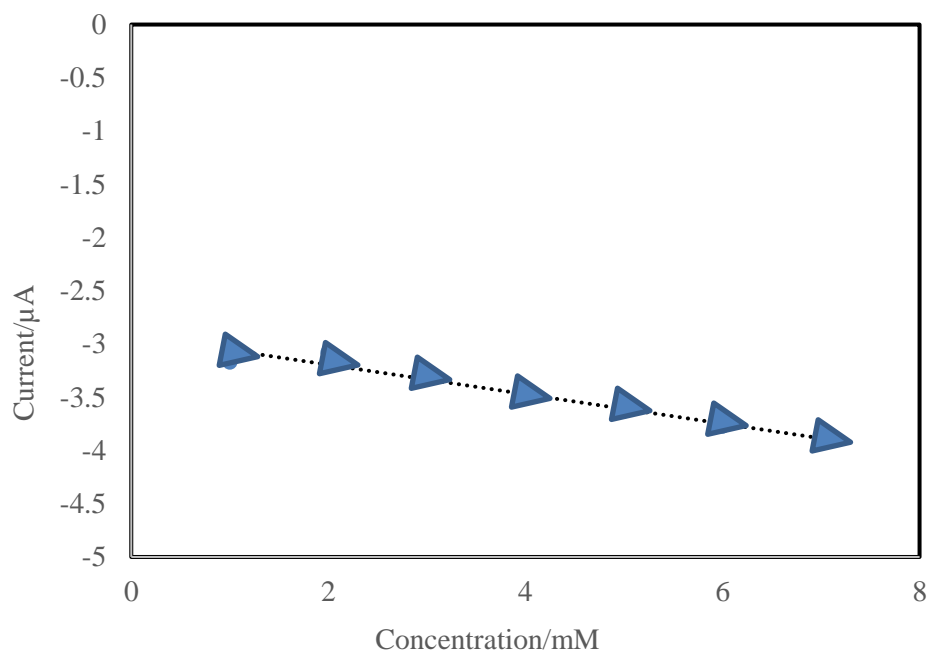


Fig. 4.15: (b) amperometric current response of The plot of concentration effect current density vs. the corresponding concentration of H₂O₂.

Tin oxide nanoclusters tend to be in more reduced state at negative potentials, which may facilitate the reduction of H₂O₂. Fig. 4.15(a) shows a typical amperometric response of the SnO₂ modified 3B pencil graphite electrode upon the successive addition of a certain concentration of H₂O₂ into stirred 0.1 M PBS (pH =7.4) solution. At the applied potential of -0.4 V, the SnO₂ modified 3B PGE gave a poor signal. Standard deviation has been calculated for each measurement and has been shown in Figure 4.15(b).

Figure: 4.16(a) shows current response at SnO₂-rGO/PGE to successive increases of H₂O₂ concentration in continuously stirred 0.1 M PBS (pH=7.4) at a potential of -0.4V.

The corresponding calibration curve, Figure 4.16(b), represents a linear current response proportional to H₂O₂ concentration with sensitivity of 0.534 (n=4) mA mM⁻¹ cm⁻² (correlation coefficient R²=0.999) and detection limit (signal/noise=3) of 0.09 μM. This fast response to H₂O₂ indicates that the SnO₂-rGO/PGE can be used for quantitative analysis of H₂O₂ in real time for various reactions involving it.

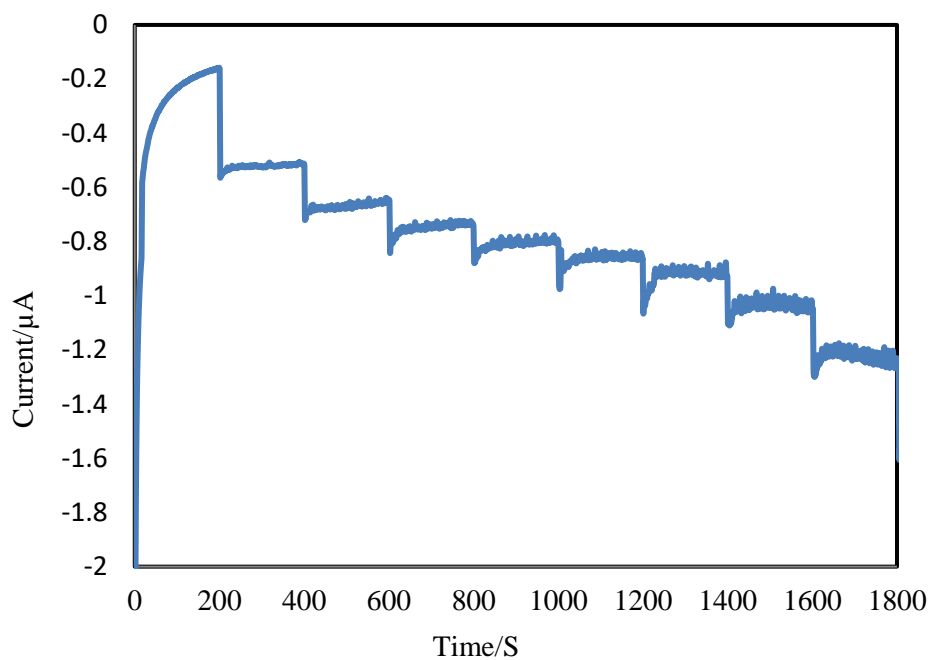


Fig. 4.16: (a) amperometric current response of the SnO₂-GO modified 3B PGEs upon the successive injection of H₂O₂ with concentrations from 1mM to 8 mM into a stirred at E_{app}= -0.4V 0.1 M PBS pH 7.4.

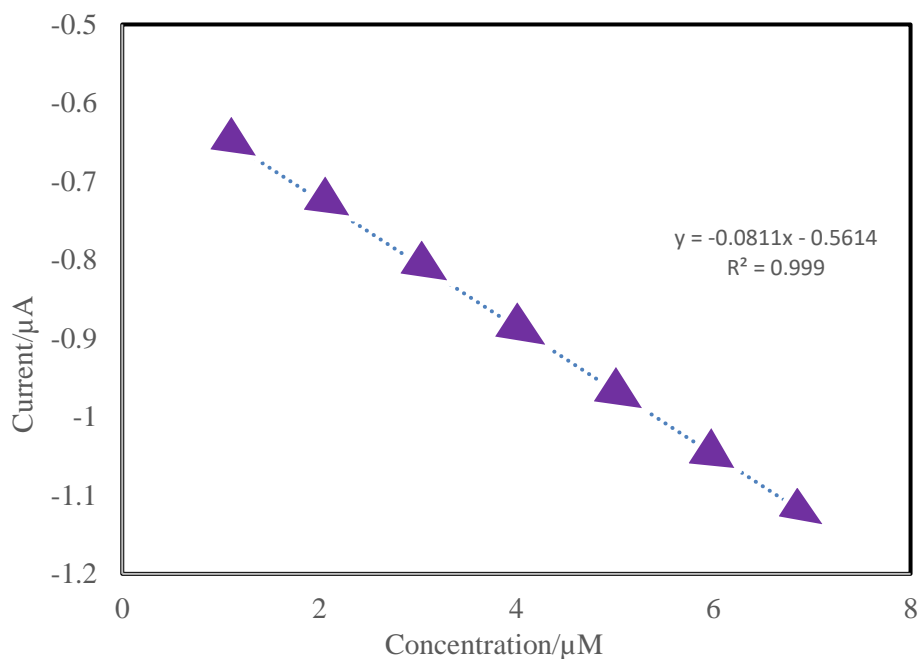


Fig. 4.16: (b) The plot of concentration effect current density vs. the corresponding concentration of H₂O₂.

4.6. Conclusions

In this study, we shown 3B pencil graphite electrodes has given good catalytic activity towards catalytic activity. The sensitivity has been found to be $0.534 \mu\text{A}/\text{mM}/\text{cm}^2$, and exhibited linear behavior for chlorine detection in the concentration range up to 6 mM although it give linear behavior more than 6 mM with a limit of detection of $0.09 \mu\text{M}$.

CHAPTER V

Conclusions

In summary, SnO₂ nanoclusters have successfully been fabricated using a hydrothermal process, and rGOs are synthesized by two step modified hummers methods. The prepared nano mixer was then studied as electrochemical sensing material for the detection of H₂O₂. Because of the high dispersion of SnO₂ nanoclusters on rGO and the synergistic effect between SnO₂ nanoclusters and rGO, the mixer exhibited excellent electro-catalytic properties towards H₂O₂ reduction and high electron transfer efficiency at the electrode/electrolyte interface. By using the SnO₂-rGO mixer as electrochemical sensing materials, highly sensitive and selective detection of H₂O₂ was achieved with a relatively low detection limit of 0.09 μM, wide linear detection range of 1-7 mM and a fast response time of 3 s. The present study indicates that SnO₂-rGO mixer represents a promising sensing material for nonenzymatic amperometric detection of H₂O₂.

Recommendations

As a recommendation,

- further work will be done on developing sensing materials, so that reduction potential of H₂O₂ can be reduced further to avoid possible interference.
- planning to enhance the stability and sensitivity of the developed sensor.
- extensive fundamental electrochemical properties of our developed sensor need to be investigated.
- development of a low-cost fabrication- process technologies to detect H₂O₂.

REFERENCES

1. C. H. Hamann, A. Hamnett, W. Vielstich., 2007, *Electrochemistry*, second edition., Wiley VCH Verlag GmbH & Co, Weinheim.
2. B. Scrosati., 2011, “3D modelling and study of electrochemical characteristics and thermal stability of commercial accumulator by simulation methods”. *J. Solid State Electrochem.*, Vol. 15, P. 1623.
3. J. Vetter, P. Novak, M.R. Wagner, C. Veit, K.C. Moller, J.O. Besenhard, M. Winter, M. Wohlfahrt-Mehrens, C. Vogler, A. Hammouche., 2005, *J. Power Sor.*, Vol. 147, P. 269.
4. C. R. Martin, and D. T. Mitchell., 1998, “Nanomaterial’s in analytical chemistry”. *Anal. Chem.*, Vol. 70, P. 322.
5. H. S. Nalwa., 1999, “Handbook of nanostructured materials and nanotechnology”. San Diego Academic Press, Vol. 4, P. 621.
6. S. Y. Chang, L. Liu, and S. A. Asher, 1994, “Preparation and properties of tailored morphology.” *J. Am. Chem. Soc.*, Vol.116, P.6739.
7. S. Santra, K. Wang, R. Tapeç, and W. Tan, 2001, “Development of novel dye-doped silica nanoparticles for biomarker application.” *J Biomed Opt.*, Vol.6, P. 160.
8. P. Couvreur, C. Dubernet, and F. Puisieux, 1995, “Polymeric drug nanoparticles prepared by an aerosol flow.” *J. Eur. Pharm Biopharm.*, Vol. 41, P. 13.
9. Tadros, T. F., 1993, “Polymer lattices, Science and technology.” (Second Edition), *Adv. Colloid Interface Sci.* Vol. 461, P. 47.
10. M. Jing, W. Li, Z. X. Zhuang, X. Chen, and X. R. Wang., 2002, “Molecular Imprinting Science and Technology.” *J. Chin. Sens. Act.* Vol. 5, P. 275.
11. J. Ju, W. Chen, 2015, “In situ growth of surfactant-free gold nanoparticles on nitrogen-doped graphene quantum dots for electrochemical detection of hydrogen peroxide in biological environments”, *Anal. Chem.*, Vol.87, P. 1903.
12. S.H. Chen, R. Yuan, Y.Q. Chai, F.X. Hu, 2013, “Electrochemical sensing of hydrogen peroxide using metal nanoparticles: a review”, *Microchim Acta*, Vol. 180, P. 32.
13. M. Giorgio, M. Trinei, E. Migliaccio, P.G. Pelicci, 2007, “Hydrogen peroxide: a metabolic byproduct a common mediator of ageing signals”, *Nat Rev Mol Cell Biol*, Vol. 8, P. 722.
14. L. G. Zamfir, L. Rotariu, V. E. Marinescu, X. T. Simelane, P. G. L. Baker, E. I. Iwuoha, et al., 2016, “Non-enzymatic polyamic acid sensors for hydrogen peroxide detection, *Sensors and Actuators B: Chemical*”, Vol. 226, P. 525.
15. A. Louvet, P. Mathurin, 2015, “Alcoholic liver disease: mechanisms of injury and targeted treatment”, *Nat Rev Gastroenterol Hepatol*, Vol. 12, P. 231.
16. U. Szkuclarek, L. Maria, M. Kasielski, S. Kaucka, D. Nowak, 2003, “Exhaled hydrogen peroxide correlates with the release of reactive oxygen species by blood phagocytes in healthy subjects, *Respiratory Medicine*”, Vol. 97, P. 718.
17. Z. Matharu, J. Enomoto, A. Revzin, 2013, “Miniature enzyme-based electrodes for detection of hydrogen peroxide release from alcohol-injured hepatocytes”, *Anal Chem*, Vol. 85, P. 932.

REFERENCES

18. J.P.E. Spencer, A. Jenner, O.I. Aruoma, C.E. Cross, R. Wu, B. Halliwell, 1996, "Oxidative DNA damage in human respiratory tract epithelial cells. Time course in relation to DNA strand breakage", *Biochem Bioph Res Co*, Vol. 224, P. 17.
19. H.M. Bolt, 2012, "Enzymic detoxification of endogenously produced mutagenic carcinogens maintaining cellular homeostasis, the cellular response to the genotoxic insult: the question of threshold for genotoxic carcinogens", *The Royal Soc. of Chem.*, Chapter 5, P. 65.
20. C. C. Kuo, W. J. Lan, C. H. Chen, 2014, "Redox preparation of mixed-valence cobalt manganese oxide nanostructured materials: highly efficient noble metal-free electrocatalysts for sensing hydrogen peroxide", *Nanoscale*, Vol. 6, P. 334.
21. D. Pramanik, S. G. Dey, 2011, "Active site environment of heme-bound amyloid β peptide associated with Alzheimer's disease", *J. Am. Chem. Soc.*, Vol.133, P. 81.
22. F. Piraino, F. Volpetti, C. Watson, S. J. Maerkl, 2016, "A digital-analog microfluidic platform for patient-centric multiplexed biomarker diagnostics of ultralow volume samples", *ACS Nano*, Vol. 10, P. 1699.
23. S. Kou, D. Cheng, F. Sun, I.M. Hsing, 2016, "Microfluidics and microbial engineering", *Lab on a chip*, Vol. 16, P. 432.
24. N. Mukhitov, J.M. Spear, S.M. Stagg, M.G. Roper, 2016, "Interfacing microfluidics with negative stain transmission electron microscopy", *Anal Chem*, Vol. 88, P. 629.
25. X. Jia, S. Dong, E. Wang, 2016, "Engineering the bio-electrochemical interface using functional nanomaterials and microchip technique toward sensitive and portable electrochemical biosensors", *Biosen. Bioelectron.*, Vol. 76, P. 80.
26. J.P. Lafleur, A. Jönsson, S. Senkbeil, J.P. Kutter, 2016, "Recent advances in lab-on-a-chip for biosensing applications", *Biosen. Bioelectron.*, Vol. 76, P. 213.
27. D.G. Rackus, M.H. Shamsi, A.R. Wheeler, 2015, "Electrochemistry, biosensors and microfluidics: a convergence of fields", *Chem. Soc. Rev.*, Vol. 44, P. 5320.
28. B. Zhou, X. Xiao, T. Liu, Y. Gao, Y. Huang, W. Wen, 2016, "Real-time concentration monitoring in microfluidic system via plasmonic nanocrescent arrays", *Biosens. Bioelectron.*, Vol. 77, P. 385.
29. E. Zor, M. E. Saglam, I. Akin, A. O. Saf, H. Bingol, M. Ersoz, 2014, "Green synthesis of reduced graphene oxide/nano-polypyrrole composite: characterization and H₂O₂ determination in urine", *RSC Advances*, Vol. 4, P. 12466.
30. Y. Peng, Z. R. Yan, Y. Wu, J. W. Di, 2015, "AgAuPt nanocages for highly sensitive detection of hydrogen peroxide", *RSC Adv.*, Vol. 5, P. 7859.
31. K. N. Han, C. A. Li, M. P. N. Bui, X. H. Pham, B. S. Kim, Y. H. Choa, et al., 2013, "On-chip electrochemical detection of bio/chemical molecule by nanostructures fabricated in a microfluidic channel", *Sens. Actuat. B*, Vol. 177, P. 472.
32. P. M. Valencia, E. M. Pridgen, M. Rhee, R. Langer, O. C. Farokhzad, R. Karnik, 2013, "Microfluidic platform for combinatorial synthesis and optimization of targeted nanoparticles for cancer therapy", *ACS Nano*, Vol. 7, P. 10680.
33. E. Swanepoel, D. E. Villiers, M. M. Dupreez, 1996; "J. Chromat. A". Vol. 729, P. 291.
34. E. Valero, F. G. Carmana, 1998, "Engineered cytokine derivatives for targeted cancer immunotherapy", *Anal. Biochem.*, Vol. 259, P. 265.

REFERENCES

35. J. Hill, 2001, "A Vertical Empire: The History of the UK Rocket launch and Space Programme", P. 1971.
36. J. Brauer, Georg, ed. 1963, "Handbook of preparative inorganic chemistry. 1. Translation editing by Reed F. (2nd ed.). New York, N.Y.: Academic Press" P. 140.
37. J. Hunt, H. Robert, A. Robert, C. Wilbur, T. Karl, 1965, "Internal-Rotation in hydrogen peroxide: the far-infrared spectrum and the determination of the hindering potential", *J. Chem. Physics*. Vol. 42 (6), 1931.
38. J. Dougherty, A. Dennis, V. Eric, 2005, "Modern Physical Organic Chemistry". University Science. Vol. 9, P. 122.
39. J. C. Martin, M. Jose, B. Brieva, Gema; Fierro, L. Jose., 2006, "Hydrogen peroxide synthesis: an outlook beyond the anthraquinone process", *Angew. Chem. International Edition*. Vol. 45, P. 6962.
40. J. Petrucci, H. Ralph, 2007, "General Chemistry: Principles & Modern Applications (9th ed.)", Prentice Hall. Vol. 2, P. 606.
41. J. Ravikumar, C. Benoit, B. Delpon, J. Bégué, J. Pierre, 2003, "Mild and selective oxidation of sulfur compounds in trifluoroethanol: diphenyldisulfide and methyl phenyl sulfoxide", *Org. Synth*. Vol. 80, P. 184.
42. J. Xu, W. Li, Y. Zhang, Q. Zhu, 2004, "A Selective, Convenient, and Efficient Conversion of Sulfides to Sulfoxides", *Synthesis*, Vol. 2, P. 227.
43. G. S. Wilson, and R. Gifford., 2005, "Biosensors for real-time in vivo measurements." *Biosens. Bioelectron*, Vol. 20, P. 2388.
44. B. R. Eggins., 2008, *Chem. Sens. Biosens.* (Google eBook), John Wiley & Sons.
45. M. Adibi, P. Hamedani, and P. Norouzi, 2011, "Copper nano-composite potentiometric sensor", *Int. J. Electrochem. Sci.*, Vol. 6, P. 717.
46. D. S. Silvester., 2011, "Recent Advances in the use of Ionic Liquids for Electrochemical Sensing," *Analyst*, Vol. 136, P. 4871.
47. Y. Ni and S. Kokot., 2008, "Does chemo metrics enhance the performance of electroanalysis," *Anal. Chim. Acta*, Vol. 626, P. 130.
48. H. Velez, 2006, "Nanowires and 1D arrays fabrication: An overview," *Thin Solid Films.*, Vol. 495, P. 51.
49. U. Yogeswaran, and S. M. Chen., 2007, "Multi-walled carbon nanotubes with poly(methylene blue) composite film for the enhancement and separation of electro-analytical responses of catecholamine and ascorbic acid", *Sens, Act. B* 128, Vol. 22, P. 1345.
50. J. W. Shie, U. Yogeswaran, and S. M. Chen., 2008, "Electroanalytical properties of cytochrome by direct electrochemistry on multi-walled carbon nanotubes incorporated with DNA biocomposite film", *Talanta*, Vol. 74, P. 1659.
51. R. W. Murray., 1984, "Chemically Modified Electrodes," *Electro. Chem.*, Vol. 13, P. 379.
52. R. P. Buck, H. Freiser, and N. Y. Plenum., 1978, "Theory and Principles of Membrane Electrodes," Chapt. 1, *Ion-Selective Electrodes in Anal. Chem.*, Vol. 1, P. 9.

REFERENCES

53. J. W. Ross, J. H. Riseman, and J. A. Krueger., 1973, "Carbon Substrate Ion Selective Electrodes", *Pure Appl. Chem.*, Vol. 36, P. 473.
54. L. C. Clark, *Trans. Am. SOC. and Artif*, 1956, History of blood gas analysis. IV. Leland Clark's oxygen electrode, *Int. Organs.*, Vol. 2, P. 41.
55. J. Janata, and R. J. Huber., 1985, "Solid State Chemical Sensors," Academic Press, Vol. 90, P. 691.
56. R. Alkire, Kolb, D. and J. Lipkowski, 2009, "Chemically modified electrodes", Germany: Wiley-VCH, Weinheim. Vol. 131, P. 13224.
57. R. Murray, W., and Albery, W. J., 1981, "Modified Electrodes: Chemically Modified Electrodes for Electro-catalysis," *The Royal Soc. Chem.*, P. 253.
58. P. D'Orazio, 2003, "Biosensors in clinical chemistry." *Clin. Chim. Acta.*, Vol. 334, P. 41.
59. R. Durst, A. Baumner, R. Murray, R. Buck, and C. Andrieux, 1997, "Chemically modified electrodes: Recommended terminology and definitions", *IUPAC*, Vol. 0, P. 1317.
60. Colorado State University Fort Collins Department of Chemistry, 1994, Chemically modified electrodes. (online version)
61. B. Sanghav, and A. Srivastava, 2010, "Simultaneous voltammetric determination of acetaminophen, aspirin and caffeine using an in situ surfactant-modified multiwalled carbon nanotube paste electrode", *Electrochimica Acta.*, Vol. 55, P. 8638.
62. B. Krajewska, 2004, "Application of chitin and chitosan-based materials for enzyme immobilizations: a review," *Enzyme Microb. Technol.*, Vol. 35, P.126.
63. [https://en.wikipedia.org/wiki/Double_layer_\(surface_science\)](https://en.wikipedia.org/wiki/Double_layer_(surface_science)).
64. J. Wang, 2000, *Anal. Electrochem.* 2nd ed., Wiley-VCH, New York.
65. R. D. Jones, M. R. Neuman, G. Sanders, and F. T. Cross, 1982, "Miniature antimony pH electrodes for measuring gastro esophageal reflux." *Ann. Thoracic Surg.*, Vol. 33, P. 491.
66. V. S. Bagotsky., 2005, "Fundamentals of Electrochemistry." John Wiley & Sons. Vol. 0, P. 719.
67. www.electrochemistry.co.kr/mall1/m_mall_detail.Php?Ps_goid=259.
68. C. Amatore, S. Arbault, D. Bruce, P. de Oliveira, M. Erard, M. Vuillaume, 2001, "Characterization of the electrochemical oxidation of peroxyxynitrite: Relevance to oxidative stress bursts measured at the single cell level", *Chem.-Eur. J.*, Vol. 7, P. 4171.
69. H. S. R. Sarathy, M. Mohseni, 2007, "The impact of UV/H₂O₂ advanced oxidation on molecular size distribution of chromophoric natural organic matter", *Environ. Sci. Technol.*, Vol. 41, P. 8315.
70. S. H. Chen, R. Yuan, Y. Q. Chai, F. X. Hu, 2013, "Electrochemical sensing of hydrogen peroxide using metalnanoparticles: a review", *Microchim. Acta*, Vol. 180, P. 32.
71. H. E. Zittel, and F. J. Miller., 1965, "A Glassy-Carbon Electrode for Voltammetry". *Anal. Chem.* Vol. 37, P. 200.

REFERENCES

72. K. Vytrás, I. Švancara, and R. Metelka., 2009, “Carbon paste electrodes in electrochemical chemistry”, *J. Serb. Chem. Soc.*, Vol. 74, P. 1021.
73. K. C. Honeychurch., 2012, “Screen-printed electrochemical sensors and biosensors for monitoring metal pollutants”, *Int. Sc. J.*, Vol. 2, P. 51.
74. A. M. bond., P. J. Mahon., J. Schiewe, and V. Vicente-Beckett., 1997, “Development of a novel and cost-effective redox sensor for voltammetric determination of pantoprazole sodium during pharmacokinetic studies”. *Anal. Chim. Acta*, Vol. 345, P. 67.
75. D. King, j. Friend, and J. Kariuki, 2010, “Pencil graphite electrodes: a versatile tool in electroanalysis”. *J. Chem. Ed.*, Vol. 87, P. 507.
76. J. K. Kariuki, 2012, “An electrochemical and spectroscopic characterization of pencil graphite electrodes”, *J. Electrochem. Soc.*, Vol. 159, P. 747.
77. N. Kurra, and G. U. Kulkarni, 2013, *Lab Chip*, Vol. 13, P. 2866.
78. N. Kurra, and G. U. Kulkarni., 2013, “Pencil-on-paper: electronic devices”, *Lab Chip*, Vol. 13, P. 2866.
79. R. L. McCreery, 2008, “Advanced carbon electrode materials for molecule”. *Electrochem.*, Vol. 108, P. 2646.
80. J. B. Jia, D. Kato, R. Kurita, Y. Sato, K. Maruyama, K. Suzuki, S. Hirono, T. Ando, O. Niwa, 2007, “Electrochemical determination of oxidative damaged dna with high sensitivity and stability using a nanocarbon film”, *Anal. Chem.*, Vol. 79, P. 98.
81. O. Niwa, J. Jia, Y. Sato, D. Kato, R. Kurita, K. Maruyama, K. Suzuki, S. Hirono, 2006, “Advanced carbon electrode materials for molecular electrochemistry”, *J. Am. Chem. Soc.*, Vol. 128, P. 7144.
82. M. Zhou, Y. M. Zhai, S. J. Dong., 2009, “Electrochemical performance of angstrom level flat sputtered carbon film consisting of sp^2 and sp^3 mixed bonds”. *Anal. Chem.*, Vol. 81, P. 5603.
83. R. L. McCreery., 2008, “Advanced carbon electrode materials for molecular electrochemistry”, *Chem. Rev.*, Vol. 108, P. 2646.
84. N. G. Shang, P. Papakonstantinou, M. McMullan, M. Chu, A. Stamboulis, A. Potenza, S. S. Dhesi, H. Marchetto., 2008, “Catalyst-free efficient growth, orientation and biosensing properties of multilayer graphene nanoflake films with sharp edge planes”. *Adv. Funct. Mater.*, Vol. 18, P. 3506.
85. M. Zhou, Y. M. Zhai, S. J. Dong, 2009, “Electrochemical sensing and biosensing platform based on chemically reduced graphene oxide”. *Anal. Chem.*, Vol. 81, P.5603.
86. M. Zhou, Y. M. Zhai, S. J. Dong, 2009, “Electrochemical sensing and biosensing platform based on chemically reduced graphene oxide”. *Anal. Chem.*, Vol. 81, P. 5603.
87. S. L. Yang, D. Y. Guo, L. Su, P. Yu, D. Li, J. S. Ye, L. Q. Mao, 2009, “Graphene based electrochemical sensors and biosensors”, *Electrochem. Commun.*, Vol. 11, P. 1912.
88. W. J. Lin, C. S. Liao, J. H. Jhang, Y. C. Tsai, 2009, *Electrochem. Commun.*, Vol. 11, P. 2153.

REFERENCES

89. L. H. Tang, Y. Wang, Y. M. Li, H. B. Feng, J. Lu, J. H. Li, 2009, "Fast synthesis of SnO₂/graphene composites by reducing graphene oxide with stannous ions". *Adv. Funct. Mater.*, Vol. 19, P. 2782.
90. N. G. Shang, P. Papakonstantinou, M. McMullan, M. Chu, A. Stamboulis, A. Potenza, S. S. Dhesi, H. Marchetto, 2008, "Catalyst-free efficient growth, orientation and biosensing properties of multilayer graphene nanoflake films with sharp edge planes", *Adv. Func. Mat.*, Vol. 18, P. 3506.
91. R. S. Nicholson, 1965, "Theory and application of cyclic voltammetry for measurement of electrode reaction kinetics". *Anal. Chem.*, Vol. 37, P. 1351.
92. A. E. Fischer, Y. Show, G. M. Swain., 2004, "Electrochemical activation of diamond microelectrodes: implications for the in vitro measurement of serotonin in the bowel", *Anal. Chem.*, Vol. 76, P. 2553.
93. Y. Shao, J. Wang, H. Wu, J. Liu, Ilhan , Aksay, Y. Lina, 2010, "Graphene based electrochemical sensors and biosensors: a review", *Electroanal.*, Vol. 22, P. 1027.
94. A. K. Geim, K. S., 2007, "The rise of graphene", *Nat. Mat.*, Vol. 6, P. 183.
95. C. S. Shan, H. F. Yang, J. F. Song, D. X. Han, A. Ivaska, L. Niu., 2009, "Direct electrochemistry of glucose oxidase and biosensing for glucose based on graphene", *Anal. Chem.*, Vol. 81, P. 2378.
96. Z. J. Wang, X. Z. Zhou, J. Zhang, F. Boey, H. Zhang, 2009, "Direct electrochemical reduction of single-layer graphene oxide and subsequent functionalization with glucose oxidase", *J. Phys. Chem.*, Vol. 113, P. 14071.
97. X. H. Kang, J. Wang, H. Wu, A. I. Aksay, J. Liu, Y. H. Lin., 2009, "Glucose oxidase-graphene-chitosan modified electrode for direct electrochemistry and glucose sensing", *Biosens. Bioelectron.*, Vol. 25, P. 901.
98. Y. Shao, J. Wang, H. Wu, J. Liu, Y. Lina, 2010, "Graphene based electrochemical sensors and biosensors: a review", *Electroanal.*, Vol. 22, P. 1027.
99. M. Zhou, Y. M. Zhai, S. J. Dong, 2009, "Electrochemical sensing and biosensing platform based on chemically reduced graphene oxide". *Anal. Chem.*, Vol. 81, P. 5603.
100. J. Wang, 2005, "Carbon nanotubes architectures in electroanalysis", *Electroanal.*, Vol. 17, P. 7.
101. L. H. Tang, Y. Wang, Y. M. Li, H. B. Feng, J. Lu, J. H. Li, 2009, "Fast synthesis of SnO₂/graphene composites by reducing graphene oxide with stannous ions", *Adv. Funct. Mater.*, Vol. 19, P. 2782.
102. W. J. Lin, C. S. Liao, J. H. Jhang, Y. C. Tsai, 2009, *Electrochem. Comm.*, Vol. 11, P. 2153.
103. C. E. Banks, R. R. Moore, T. J. Davies, R. G. Compton, 2004, "Investigation of modified basal plane pyrolytic graphite electrodes: definitive evidence for the electrocatalytic properties of the ends of carbon nanotubes", *Chem. Comm.*, Vol. 1804. P. 98.

REFERENCES

104. M. Pumera, R. Scipioni, H. Iwai, T. Ohno, Y. Miyahara, M. Boero, 2009, "Graphene based electrochemical sensors and biosensors: a review", *Chem. Eur. J.*, Vol. 15, P. 10851.
105. N. G. Shang, P. Papakonstantinou, M. McMullan, M. Chu, A. Stamboulis, A. Potenza, S. S. Dhesi, H. Marchetto, 2008, *Adv. Funct. Mater.*, Vol. 18, P. 3506.
106. S. Alwarappan, A. Erdem, C. Liu, C. Z. Li, 2009, "Probing the electrochemical properties of graphene nanosheets for biosensing applications". *J. Phys. Chem. C.*, Vol. 113, P. 8853.
107. Y. Wang, Y. M. Li, L. H. Tang, J. Lu, J. H. Li, 2009, "Electron transfer mechanism of cytochrome cc at graphene electrode". *Electrochem. Commun.*, Vol. 11, P. 889.
108. G. D. Liu, Y. H. Lin, 2006, "Functionalized carbon nanotubes and nanofibers for biosensing applications". *Electrochem. Commun.*, Vol. 8, P. 251.
109. L. Wu, X. J. Zhang, H. X. Ju, 2007, "Amperometric sensor for ethanol based on one-step electropolymerization of thionine-carbon nanofiber nanocomposite containing alcohol oxidase", *Biosens. Bioelectron.*, Vol. 23, P. 479.
110. M. Zhou, L. Shang, B. L. Li, L. J. Huang, S. J. Dong, 2008, "Graphene based electrochemical sensors and biosensors", *Biosens. Bioelectron.*, Vol. 24, P. 442.
111. C. S. Shan, H. F. Yang, D. X. Han, Q. X. Zhang, A. Ivaska, L. Niu, 2009, "Graphene/AuNPs/chitosan nanocomposites film for glucose biosensing", *Biosens. Bioelectron.*, Vol. 25, P. 1070.
112. H. Wu, J. Wang, X. H. Kang, C. M. Wang, D. H. Wang, J. Liu, I. A. Aksay, Y. H. Lin, 2009, "Glucose biosensor based on immobilization of glucose oxidase in platinum nanoparticles/graphene/chitosan nanocomposite film", *Talanta.*, Vol. 80, P. 403.
113. A. Sassolas, B. D. Leca-Bouvier, L. J. Blum, 2008, "DNA biosensors and microarrays", *Chem. Rev.*, Vol. 108, P. 109.
114. J. Li, S. J. Guo, Y. M. Zhai, E. K. Wang, 2009, "High-sensitivity determination of lead and cadmium based on the Nafion-graphene composite film". *Anal. Chim. Acta.*, Vol. 649, P. 196.
115. J. Li, S. J. Guo, Y. M. Zhai, E. K. Wang, 2009, "Preparation of novel carbon-based nanomaterial of graphene and its applications electrochemistry", *Electrochem. Commun.*, Vol. 11, P. 1085.
116. G. Kefala, A. Economou, A. Voulgaropoulos, 2009, "A study of Nafion-coated bismuth-film electrodes for the determination of trace metals by anodic stripping voltammetry", *Analyst*, Vol. 129, P. 1082.
117. L. D. Zhu, C. Y. Tian, R. L. Yang, J. L. Zhai, 2008, "Graphene based electrochemical sensors and biosensors", *Electroanal.*, Vol. 20, P. 527.
118. H. Xu, L. P. Zeng, S. J. Xing, Y. Z. Xian, G. Y. Shi, 2008, "Graphene based electrochemical sensors and biosensors: a review", *Electroanal.*, Vol. 20, P. 2655.
119. P. Wu, Z. Cai, Y. Gao, H. Zhang, C. Cai, 2011, "Enhancing the electrochemical reduction of hydrogen peroxide based on nitrogen doped graphene for measurement of its releasing process from living cells", *Chem. Commun.*, Vol. 47, P. 11327.

REFERENCES

120. D. O. Fea, D. Araujo., 2015, "Layer-by-layer films based on biopolymers extracted from red seaweeds and polyaniline for applications in electrochemical sensors of chromium VI", *Mater. Sci. Eng.*, Vol. 20, P. 9.
121. Y. Zhang, X. Bai, X. Wang, KK. Shiu, Y. Zhu, H. Jiang., 2014, "Highly sensitive graphene-Pt nanocomposites amperometric biosensor and its application in living cell H₂O₂ detection", *Anal. Chem.*, Vol. 86, P. 9459.
122. H. Fang, Y. Pan, W. Shan, M. Guo, Z. Nie, Y. Huang, S. Yao., 2014, "Enhanced non-enzymatic sensing of hydrogen peroxide released from living cells based on Fe₃O₄/self-reduced graphene nanocomposites", *Anal. Meth.*, Vol. 6, P. 6073.
123. L. Kong, Z. Ren, N. Zheng, S. Du, J. Wu, J. Tang, H. Fu, 2015, "Interconnected 1D Co₃O₄ nanowires on reduced graphene oxide for enzymeless H₂O₂ detection". *Nano Res.*, Vol. 8, P. 469.
124. X. Li, M. Xu, H. Chen, J. Xu, 2015, "Bimetallic Au@Pt@Au core shell nanoparticles on graphene oxide nanosheets for high performance H₂O₂ bi-directional sensing", *J. Mater. Chem.*, Vol. 3, P. 4355.
125. S. K. Maji, S. Sreejith, A. K. Mandal, X. Ma, Y. Zhao., 2014, "Immobilizing gold nanoparticles in mesoporous silica covered reduced graphene oxide: a hybrid material for cancer cell detection through hydrogen peroxide sensing". *ACS. Appl. Mat. Interf.*, Vol. 6, P. 13648.
126. Y. Sun, K. He, Z. Zhang, A. Zhou, H. Duan., 2015, "Real-time electrochemical detection of hydrogen peroxide secretion in live cells by Pt nanoparticles decorated graphene-carbon nanotube hybrid paper electrode", *Biosens. Bioelectron.*, Vol. 68, P. 358.
127. H. Chang, X. Wang, K. K. Shiu, Y. Zhu, J. Wang, Q. Li, B. Chen, H. Jiang., 2013, "Layer-by-layer assembly of graphene, Au and poly (toluidine blue) films sensor for evaluation of oxidative stress of tumor cells elicited by hydrogen peroxide". *Biosens. Bioelectron.*, Vol. 41, P. 789.
128. F. Xi, D. Zhao, X. Wang, P. Chen., 2013, "Non-enzymatic detection of hydrogen peroxide using a functionalized three-dimensional graphene electrode", *Electrochem. Commun.*, Vol. 26, P. 81.
129. S. Pourbeyram, and K. Mehdizadeh., 2016, "Nonenzymatic glucose sensor based on disposable pencil graphite electrode modified by copper nanoparticles", *J. Food Drug Anal.*, Vol. 24, P. 894.
130. D. E. David, M. Popa, Buleandra, Z. Moldovan, E. E. Iorgulescu, and Badea, I. A., 2016, "Pencil Graphite Electrodes: A Versatile Tool in Electroanalysis", *Anal. Meth.*, Vol. 8, P. 6537.
131. A. Erdem, P. Papakonstantinou, and H. Murphy, 2006, "Direct DNA hybridization at disposable graphite electrodes modified with carbon nanotubes", *Anal. Chem.*, Vol. 78, P. 6656.
132. N. Baig, and A. Kawde., 2015, "A novel, fast and cost effective graphene-modified graphite pencil electrode for trace quantification of L-tyrosine", *Anal. Meth.*, Vol. 7, P. 9535.
133. D. King, J. Friend, and J. Kariuki., 2010, "Pencil graphite electrodes: a versatile tool in electroanalysis", *J. Chem. Ed.*, Vol. 87, P. 507.

REFERENCES

134. M. Sajid, C. Basheer, A. Alsharaa, and Al-Ahwal, M. S., 2016, New methodology for the determination of phthalate esters, bisphenol a, bisphenol a diglycidyl ether, and nonylphenol in commercial whole milk samples”, *Anal. Chim. Acta*, Vol. 924, P. 35.
135. M. Sajid and C. Basheer, 2016, “Improvements in the vapor-time profile analysis of explosive odorants using solid-phase microextraction”, *J. Chromatogr. A*, Vol. 1455, P. 37.
136. Md. Juel Islam, 2016, “Development of sensor for free available chlorine estimation in surface water”, postgraduate Thesis, Dept. of Chemistry, KUET, Khulna, Bangladesh.
137. A. Jo, Y. Lee and C. Lee., 2017, “Real-time selective detection of hydrogen peroxide based on a tantalum deposited pencil lead electrode for evaluation of enzyme activities, *Electroanal.* 2017, Vol. 29, P. 1.
138. K. Pokpas, Jahed, N., Tovide, O., Baker, P. G. and Iwuoha, E. I., 2014, “Nafion-graphene nanocomposite in situ plated bismuth-film electrodes on pencil graphite substrates for the determination of trace heavy metals by anodic stripping voltammetry”. *Int. J. Electrochem. Sci.*, Vol. 9, P. 5092.
139. C. Zhang, L. Li, J. Ju, W. Chen, 2016; “Electrochemical sensor based on graphene supported tin oxide for nonenzymatic detection of hydrogen peroxide”. *Electrochim. Acta.*, Vol. 210, P. 181.
140. W. Zhao, H. Wang, X. Qin, X. Wang, Z. Zhao, Z. Miao, L. Chen, M. Shan, Y. Fang, Q. Chen, 2009, “A novel nonenzymatic hydrogen peroxide sensor based on multi-wall carbon nanotube/silver nanoparticle nano hybrid modified gold electrode”, *Talanta*, Vol. 80, P. 1029.